AECR7715/1064
October 20, 1977

Final Report

on

Conceptual Analyses

of

EXTENSIBLE BOOMS TO SUPPORT A SOLAR SAIL

JPL Subcontract #954700
Under NASA Contract NAS7-100

Prepared by

AEC-ABLE ENGINEERING COMPANY, INC.
P. O. Box C
Goleta, California 93017

R. F. Crawford
M. D. Benton

TABLE OF CONTENTS

LIST OF TABLES AND FIGURES

FOREWORD

This document is the final report on work performed by AEC-ABLE ENGINEERING CO., INC. (ABLE) under JPL Task Order No. RD-156, as authorized by its Modification No. 6. Mr. M. H. Jacobs is the Contract Officer and Mr. J. D. Kievit is the Responsible Engineer for JPL on this Task Order. Mr. R. F. Crawford is the Program Manager for ABLE.

INTRODUCTION AND SUMMARY

The objective of this investigation was to conceptually design and analyze extensible booms which could function as the diagonal spars and central mast of an 800-meter-square, non-rotating Solar Sailing Vehicle. A sketch of one version of the vehicle is shown in Figure 1.

The boom design concept that was investigated for this application is sketched in Figure 2. It is an extensible lattice boom which is stowed and deployed by elastically coiling and uncoiling its continuous longerons (see attached brochure for a more detailed description of this mechanism). The present investigation was restricted to the booms, themselves; their stowage-deployment canisters were investigated by JPL.

Initial designs and analyses of the diagonal spars were based on each spar being about 577 meters long and stay-supported along their lengths to provide five equal-length free-spans. The total mast length was initially taken to be equal to three free-span lengths of the spars, or 346 meters. Each inboard free-span of each spar was to withstand a maximum axial compressive load of 137.9 N with a simultaneous lateral acceleration of 0.0105 m/sec^2. All free-spans of diagonal spars

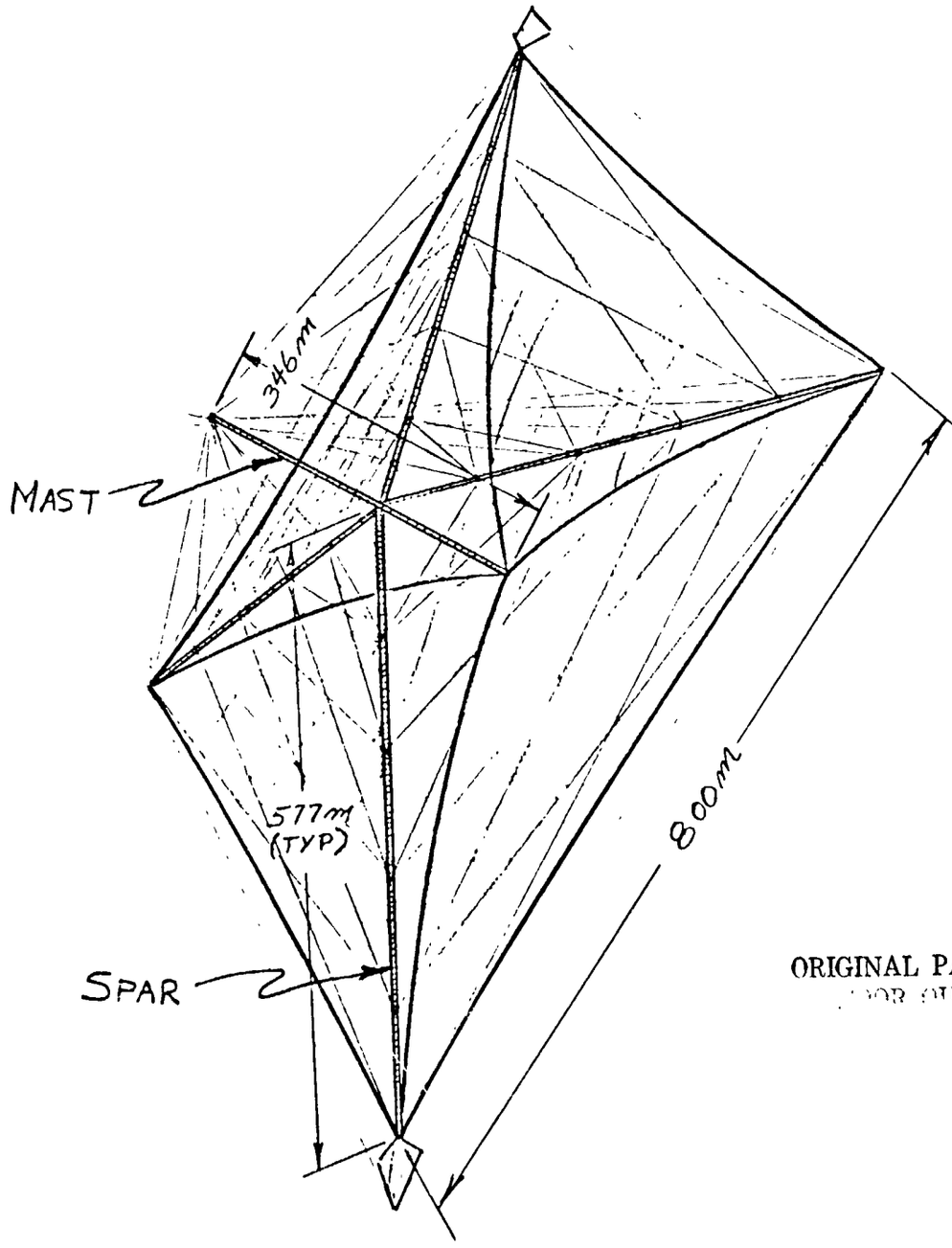

FIGURE 1 -- Initial Version of Solar Sailing Vehicle

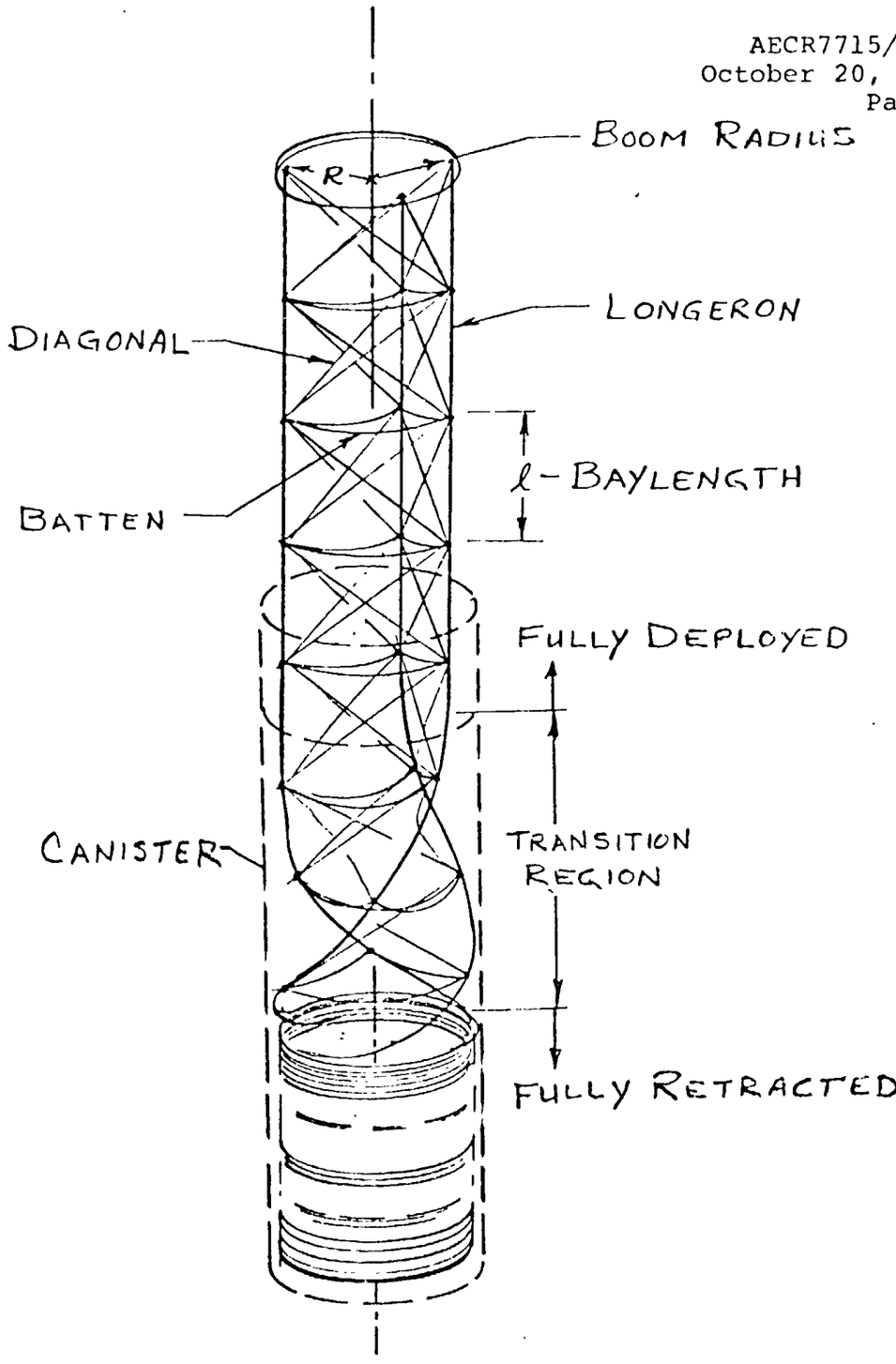

FIGURE 2 -- Coilable Lattice Boom with Stowage/Deployment Canister

and central mast were to be of the same design as that required for the more severely loaded inboard free-spans of the diagonal spars. Because the vehicle was to operate at 0.3 AU, JPL also specified that the extensible booms be capable of withstanding temperatures compatible with a sail temperature of about 580°K. This restricted candidate boom materials to those capable of withstanding a temperature approximately equal to that of the sail.

Subsequently, the investigation was repeated for an enlarged Solar Sail Vehicle with diagonal spars that were 652 meters long and with a total mast length of 374 meters. The spars were stay-supported to provide seven free-spans of differing, optimum lengths, and the mast consisted of four free-spans. As initially, all free-spans were to have the same cross sections. However, the axial compressive loads in these free-spans were significantly reduced from those of the initial investigation, while the lateral acceleration was essentially unchanged. This subsequent investigation was interactive between ABLE and JPL inasmuch as JPL iteratively computed axial loads in each of the free-spans, which changed with free-span lengths, while ABLE determined the seven different free-span lengths in each spar which would minimize the total weights of the spars and mast for the JPL-specified loads.

To define lattice boom designs that could satisfy these requirements, it was necessary to consider effects of initial

waviness of both the longerons and the overall boom assemblies. These considerations were necessary because the presence of such waviness is highly probable in the slender structures that were defined by this investigation, and because the effects of waviness on the strength of these structures was shown to be very significant.

Maximum expected amplitudes of these initial wavinesses were calculated for use in the strength analyses. These waviness calculations included effects of dimensional variations in the fabricated boom parts, joint misalignments and distortions owing to temperature gradients.

The strength of these wavy lattice booms was analyzed and shown to be characterized by an unbifurcated maximum strength, rather than by a classical bifurcated column-buckling strength. The unbifurcated maximum strength was derived by using accurate engineering approximations to represent the deformation mechanics of the booms. The resulting equations were then programmed for rapid, computerized investigations of the various loading and geometric parameters that affect the strength and minimum-weight designs of these lattice booms.

Boom weights were calculated by using a semi-empirical formulation which related the overall weight of a boom to the weight of its longerons (the latter determined from the strength requirements). Although this formulation of the overall weight

was based on prior experience with booms of different sizes and materials, subsequent detailed design studies of the selected design proved the formulation was accurate for this application.

The results of the investigation for the initially defined requirements showed that booms of either titanium tubing or HTS-Graphite/Polyimide solid rods were feasible and were the least mass among several metallic and composite materials that were considered. These two lighter-mass booms were of approximately equal mass, 0.309 kg/m. The diameter of the titanium boom was 1.168 meters, as limited by the available stowage envelope, while that of the HTS-Graphite/Polyimide boom was 0.400 meters.

JPL specified that only titanium boom designs should be considered in the subsequent investigation of the longer diagonal spars with seven free-spans. As noted earlier, JPL and ABLE iteratively varied the loads and free-span lengths of the spars. The mass of the converged final design was 0.178 kg/m. This decreased unit weight was the combined effect of decreased free-span lengths, decreased compressive loads, optimization of the individual free-span lengths and decreased allowable minimum wall thickness of the longeron tubing from 0.0203 to 0.0127 cm.

As an adjunct to these investigations, analyses were performed which showed the following weight sensitivities of the final titanium boom design:

1) Mass increases significantly with small increases in span lengths and axial loading or decreases in boom radius.

2) Mass is relatively insensitive to the magnitude of lateral inertial loading considered and to small changes from the presently estimated initial wavinesses.

3) Although reductions in boom mass are theoretic possible by geometric changes in the final boom design, cons ..i. tions of system optimization and fabricability would probably preclude such reductions.

It is concluded that realization of the final boom design is feasible; however, that realization will require technology development and demonstration in several areas which are defined.

The following sections of this report and its appendices present details of all the above-summarized design data and analyses.

DESIGN CRITERIA AND SPECIFICATIONS

Following are design criteria and specifications that were set up by JPL and ABLE to govern the initial and final phases of the conceptual design and analysis of the spars of the Solar Sailer. Initial criteria were used for preliminary sizing of candidate booms, both of metallic and composite materials. From those preliminary results a titanium construction was selected for further investigations, whose analysis and design was governed by final, modified criteria and specifications.

Initial Criteria

Dimensions -- Each spar shall be 577.4 m long, composed of five equal-length, stay-supported free-spans of 115.5 m. The central mast shall consist of three 115.5 m free-spans. All spar and mast free-spans are to be of identical construction. These spar and mast dimensions, and those for the inplane stays, are established by JPL Drawing No. 10082706, Sheet 1 of 4.

The nominal diameter of the booms (spars and masts) shall not exceed 1.168 m (46 in).

Safety Factor -- Design loads shall be defined as limit load times a safety factor of 1.25. Limit loads are those identified

to be the maximum loads expected to act on the structure. The spars and mast shall be designed such that they can withstand the design loads without failure.

Loads --

1) The design value of the maximum axial load in a spar free-span is 120 N. This load occurs in the root free-span and does not include axial loads induced by inertial loading of the inplane stays.

2) The spars and inplane stays experience a lateral acceleration of 0.0105 m/sec^2. The spars are so oriented relative to this acceleration that at the middle of each free-span the inertial loads equally compress two longerons and tension the third.

3) The design axial load induced in the root free-span of the spar by the initially loaded inplane stays is 17.9 N. The limit value of this load, 14.3 N, was calculated from the formula

$$T = T_O + \frac{AE}{24}\left(\frac{wL}{T}\right)^2$$

where T = tension in a stay under lateral acceleration

T_O = initial stay tension

AE = stay extensional stiffness

L = stay length

w = inertial loading of stay

This formula was derived by assuming the stays had a parabolic equilibrium shape in response to the inertial loading.

Values of AE and w were calculated based on titanium stays, all of which had a cross-sectional area of 0.00516 cm^3 (0.0008 in^3), specific gravity of 4.43 g/cm^3, and Young's modulus of 10.34 x 10^{10} N/m^2 (15 x 10^6 psi). T_O was taken to be 1.0 N for all the inplane stays, and their lengths were calculated from the data on JPL Drawing No. 10082706, Sheet 1 of 4.

Temperature -- Maximum operational temperature for the spars was taken to be 451°K (300°F). This was based on the JPL data

given in Figure 3. That is, the maximum boom temperature T_B was approximated as

$$T_B = \sqrt[4]{\frac{\varepsilon_T}{\varepsilon_B}}\, T_S$$

where T_S = sail temperature
= 629°K (600°F)

ε_{BF} = sail backface emissivity
= 0.27

ε_B = boom IR emissivity
= 1.0

The sail-to-longeron view factor was implicitly taken here to be 1.0.

Besides this maximum operational temperature, it was decided that the boom materials should, when not loaded, be capable of withstanding exposure to a temperature of 629°K (600°F).

Material Properties -- The materials listed in Table 1 were considered to be candidate materials for the booms. Physical and mechanical properties pertinent to the boom design are also listed in Table 1. The moduli listed are for the operational temperature of 451°K (300°F), while the strengths and strains are for room temperature.

Based on prior experience with the design of composite coilable longerons for deployable booms, the design coiling strains ε listed in Table 1 are one-half the fracture strains, for the composite materials. For the metallic materials, their combined

FIGURE 3

SAIL TEMPERATURE VS. MISSION TIME

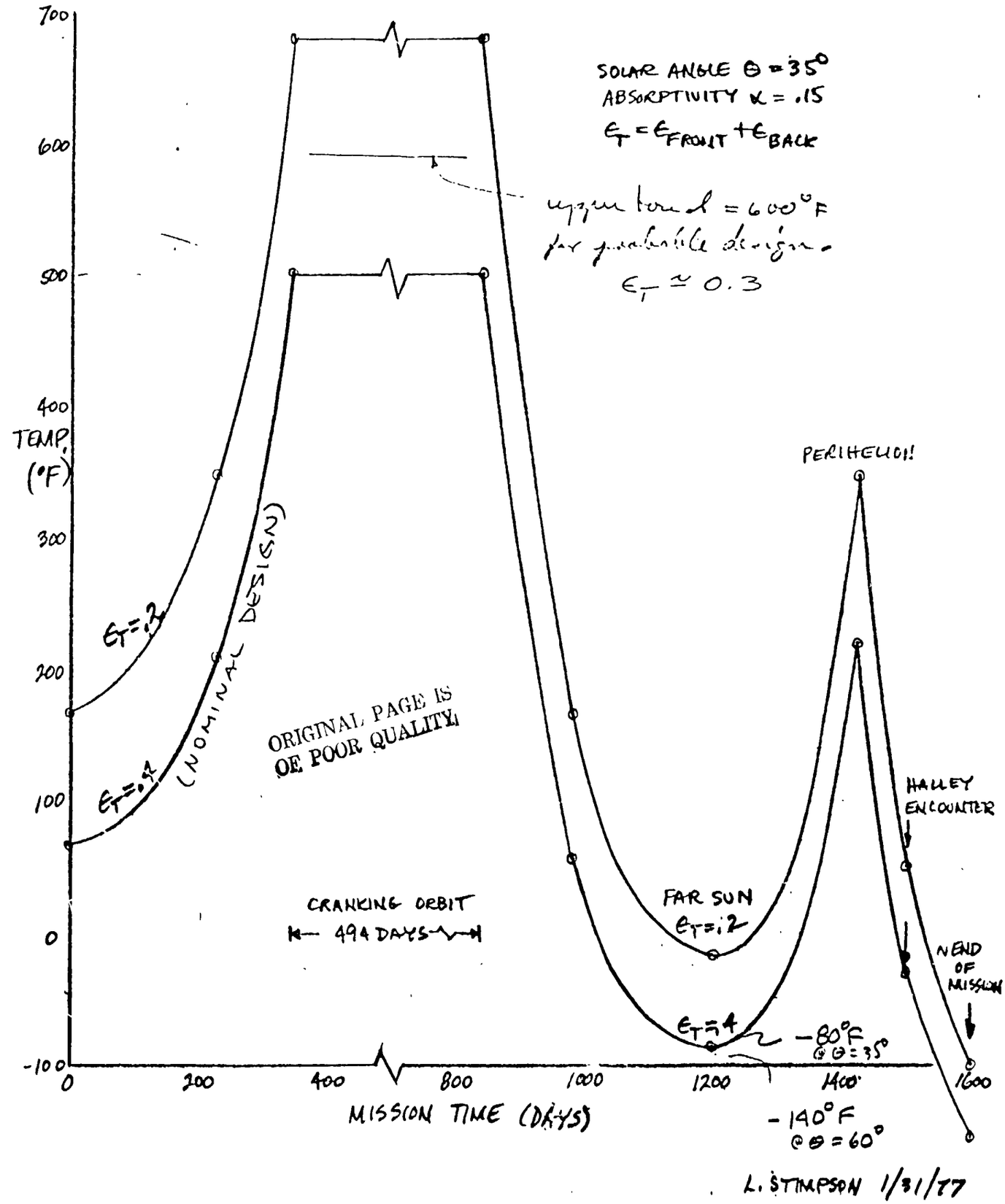

direct and shearing strengths are known with greater accuracy. Therefore, their design coiling strains are taken to be 0.8 times their proportional limit strains. The strengths and design strains listed in Table 1 are for room-temperature conditions because the boom will be coiled and uncoiled (stowed and deployed) at approximately that condition.

Initial Waviness -- The longerons of each bay of the spars and masts were assumed to have initial waviness defined by

$$y = y_\ell \sin \frac{\pi x}{\ell}$$

where y_ℓ = amplitude of longeron waviness

and ℓ = baylength

And, each free-span of the spars was assumed to have initial waviness defined by

$$y = y_L \sin \frac{\pi x}{L}$$

where y_L = amplitude of boom waviness

and L = length of spar free-spans

These waviness amplitudes were determined by making preliminary estimates of the effects of such factors as initial curvature of longeron stock, temperature gradients across and between longerons, deviations in lengths of diagonal members, splice misalignment and external forces. The result of this preliminary investigation was that the following values were selected for the waviness parameters y_ℓ/ℓ and y_L/L .

Table 1 -- MATERIALS INVESTIGATED

Material	$E \times 10^{-10}$ (N/m^2)	$\sigma \times 10^{-8}$ (N/m^2)	ϵ_{DESIGN}	Density (g/cm^3)
Ti-6Al-4V	10.34	9.10	0.00660	4.428
Steel	19.3	10.34	0.00428	7.749
7075-T6 Aluminum	6.2	4.96	0.00576	2.767
HTS Graphite/Polyimide	13.4	13.44	0.00500	1.660
HM Graphite/Polyimide	26.5	7.14	0.00135	1.600
S-Glass/Polyimide	5.69	20.00	0.01750	1.937

For metallic booms:

$$\frac{y_\ell}{\ell} = \frac{1}{2500}$$

$$\frac{y_L}{L} = \frac{1}{1000}$$

and, for composite booms:

$$\frac{y_\ell}{\ell} = \frac{1}{2000}$$

$$\frac{y_L}{L} = \frac{1}{750}$$

(Note that the above values for the metallic booms were later confirmed by the analyses presented in Appendix A.)

Weight Model -- Boom weight per unit length w_B was predicted by the following semi-empirical formula which is based on measured weights of previously fabricated booms.

$$w_B = 3w_\ell \left(1 + 1.55 \frac{R}{\ell}\right) + \frac{R}{\ell}\left(\frac{0.0697}{R} + 6w_D \sqrt{3 + \left(\frac{\ell}{R}\right)^2}\right)$$

where w_ℓ = weight per unit length of a longeron, as calculated to provide the specified boom strength

R = boom radius

ℓ = baylength

and w_D = weight per unit length of the diagonal material; taken here to be the same as the JPL-specified stay material.

In the above formula, the four terms (from left to right) are identified as,

1) Longeron weight

2) Batten weight

3) Weight of corner fittings

4) Weight of diagonal members

(Note that the accuracy of weights predicted by this formula were later verified by detail design investigations.)

Final Criteria and Specifications

Following are the modifications and additions to the "Initial Criteria and Specifications". A titanium boom construction was selected to be "baseline" as a result of the initial screening and sizing of booms of the various candidate materials. Therefore, the criteria and specifications presented below were applied only to a final analysis and design of a coilable titanium boom. The initial criteria and specifications still apply if they are not superseded by the following.

Dimensions -- Each spar of the Solar Sailer shall be approximately 652 meters long and the length of the central mast shall be approximately 374 meters. For the baseline design, each spar shall consist of seven stay-supported free-spans and the mast shall consist of four such free-spans. The lengths of the free-spans are not specified, but shall be optimized to minimize their total mass.

The arrangement and dimensions of the inplane stays for the final configuration are established by JPL Drawing No. 10082706,

Sheet 4 of 4. (Note that the cited drawing shows the finally selected, iterated span lengths.)

Although the baseline design is to have seven free-spans per spar, weight sensitivity analyses shall be performed for spars having six and eight free-spans.

Wall thicknesses of the titanium tubing selected for longerons and battens of the spars and mast shall not be less than 0.127 mm (0.005 inch).

All spar and mast free-spans must have identical cross sections, except that the mast free-spans can utilize different-size longeron tubing.

Safety Factor -- Unchanged

Loads -- Axial loads in the mast and spar free-spans shall be provided by JPL for each set of lengths of those free-spans (i.e., each distribution of specified total length) specified by ABLE. The loads provided by JPL shall not include those induced by tensions in the inplane stays. These latter loads shall be calculated by ABLE for each group of spar and mast free-span lengths that is investigated. The loads induced by the inplane stays shall be calculated by the same methods as indicated by the initial criteria and the pattern of the inplane stays is that shown on JPL Drawing No. 10082706, Sheet 4 of 4.

Thus, the final loads on the spars and mast are to be determined iteratively by JPL and ABLE interaction, so as to optimize free-span lengths and minimize their total mass.

Temperature -- The sail temperature T_S shall be 582°K (520°F) and shall have a backside (boom-side) emissivity of 0.55. The view-factor analysis given in Appendix B of this report shows that over most of the spar length, the boom temperature T_B is $0.82\ T_S$. Therefore, the design boom temperature shall be 477°K (344°F).

Material Properties -- Unchanged; including modulus for Ti-6Al-4V.

Initial Waviness -- Appendix A gives analyses of initial wavinesses for the final design of the longerons and overall booms. Those analyses essentially substantiate the preliminary estimate. Therefore, the following values for the initial waviness parameters were used to derive the final titanium boom design:

$$\frac{y_\ell}{\ell} = \frac{1}{2500}$$

$$\frac{y_L}{L} = \frac{1}{1000}$$

Weight Model -- Unchanged

STRENGTH AND DESIGN ANALYSIS

Appendix C presents equations that were developed for calculating the maximum axial load P_{MAX} that can be withstood by a lattice column, of the type shown in Figure 2, where

1) both the longerons and overall assembly of the column are initially wavy,

2) the column is simply supported at both ends of its span length L,

3) it is laterally loaded owing to acceleration of its own mass, so as to equally compress two longerons and tension the third; and,

4) the boom overall waviness can be at any angle γ relative to the direction apecified for those deflections owing to the inertial loading.

Further details of the assumptions and approximations used in the strength determination are listed in Appendix C. The equations developed there are general inasmuch as they can be applied to any longeron cross section and any boom proportions.

Example calculations presented in Appendix C show that in the presence of initial overall waviness, the maximum load-carrying capability of these columns is less than the classical buckling strength, where stable and unstable equilibrium configurations bifurcate. For these wavy columns, the effect of applying and increasing the axial load is to increase the

lateral deflection of the column, until a bent configuration is attained for which any attempt to further increase the load results in unstably increasing deflections and decreasing bending stiffness. P_{MAX} is defined as the load at that point of divergent deflections; although, the column bending stiffness at that condition would indicate a reserve of buckling strength.

The equations developed in Appendix C were used to calculate design proportions of coilable lattice booms that satisfy the "Initial" and "Final" criteria and specifications given previously. The strength equations and criteria were applied as follows.

The maximum strength of a lattice column, as formulated in Appendix C, depends on the design variables which are indicated functionally as follows:

$$P^*_{MAX} = P^*_{MAX}\left(P,\ n,\ w_B,\ L,\ E,\ y_\ell/\ell,\ y_L/L,\ \ell/R,\ R,\ \rho,\ \gamma,\ \text{and}\ \bar{\rho}_B\right)$$

All the symbols used here are defined in Appendix C, Figure 2, and the previous section of this report. To satisfy the design criteria, the variables of the strength equations were determined as follows:

P = specified design load

n = load factor

$= \frac{0.0105}{9.81} = 0.00107$

w_B = boom weight per unit length, defined by weight model

L = specified span length

E = Young's modulus as specified in Table 1

$y_\ell/\ell = \frac{1}{2500}$ and $y_L/L = \frac{1}{1000}$ for metallic booms

$y_\ell/\ell = \frac{1}{2000}$ and $y_L/L = \frac{1}{750}$ for composite booms

ℓ/R = 1; selected to ensure compact stowage geometry while maximizing longerons buckling strength

R = boom radius; as selected to minimize w_B, or as limited by specification that $2R \leq 1.168$ m

ρ = longeron radius of gyration; as selected to minimize w_B, or as limited by ε_{DESIGN} values listed in Table 1

γ = direction of overall waviness, as selected

For particular values of the above variables, the relationship between p^*_{EU} and $\bar{p}_B$ (similar to that shown on Figure C3 of Appendix C) was determined insofar as necessary to define p^*_{MAX}, where

$$p^*_{MAX} \equiv p^*_{EU}\Big|_{MAX}$$

From this definition,

$$p^*_{MAX} = \frac{P_{MAX}}{P_{EU}} = \frac{2P_{MAX}L^2}{3\pi^2 EA_\ell R^2}$$

Note that a computational subroutine was developed to calculate p^*_{MAX} with an accuracy of 0.001 (typical values of p^*_{MAX} are 0.3 to 0.7).

In the preliminary sizing of composite booms, their longerons were assumed to be square and solid, with cross-

sectional area A_ℓ given by

$$A_\ell = S^2 - 12\rho^2$$

As a trial input to a design computation, a value of R was selected such that

$$R \leq R_{LIMIT}$$

Since the longeron radius of gyration ρ is

$$\rho = \frac{S}{\sqrt{12}}$$

and the coiling strain ε is

$$\varepsilon = \frac{S}{2R} \leq \varepsilon_{DESIGN}$$

then a value of ρ was selected such that

$$\rho < \frac{R\varepsilon_{DESIGN}}{\sqrt{3}}$$

These selected values of R and ρ, along with values of the other variables as dictated by the criteria and specification, were used as input to the computer program developed to automatically make design calculations. The previously mentioned subroutine to the design program then calculated p^*_{MAX} (with $P_{MAX} = P$ and $A_\ell = 12\rho^2$) as

$$R = \sqrt{\frac{PL^2}{18\pi^2 E\rho^2 p^*_{MAX}}}$$

This latter value of R was compared to its input value and the computation was recycled with changed values of the input R until they agreed with an accuracy of $\Delta R \approx R/500$. The strain was monitored during these computations to insure

$\varepsilon \leq \varepsilon_{DESIGN}$.

Thus, values of R and S were calculated for booms whose strengths are P .

Note that when p^*_{MAX} was calculated by the subroutine for a particular set of design variables, the input value of w_B was not recalculated for each iteration cycle. The initially estimated value of w_B was used for all these iterations and then checked against the converged design value of w_B . The computation cycle was rerun only if the calculated w_B differed greatly (say 30%) from the input value of w_B . This procedure was permissible because p^*_{MAX} was quite insensitive to changes in w_B .

Sizing calculations for booms with metallic tubular longerons proceeded much the same as those outlined above for solid rods. The chief difference was that R was set equal to its design limit value because w_B was found to be minimized there. An initial value of the longeron radius of gyration was then calculated according to

$$\rho = \frac{r_o}{\sqrt{2}} = \frac{R\varepsilon}{\sqrt{2}}$$

where

$$\varepsilon \leq \varepsilon_{DESIGN}$$

This value of ρ was subsequently compared to

$$\rho = \frac{R}{\sqrt{2}}\sqrt{\varepsilon^2 - \frac{PL^2}{3\pi^3 ER^4 p^*_{MAX}}}$$

which is derived from considering that

$$A_\ell = \pi \left(r_o^2 - r_i^2\right)$$

$$\rho^2 = \frac{1}{4}\left(r_o^2 + r_i^2\right)$$

$$\varepsilon = \frac{r_o}{R}$$

and

$$\frac{A_\ell}{R^2} = \frac{2PL^2}{3\pi^2 ER^4 p^*_{MAX}}$$

For a converged value of ρ ($\Delta\rho \leq \rho/200$) the longeron inside radius is, from the preceding equations,

$$r_i = R\sqrt{\left(\frac{2\rho}{R}\right)^2 - \varepsilon^2}$$

Values of w_B were calculated for various values of ε to minimize w_B. In the initial design calculations the minimum w_B occurred for

$$\varepsilon = \varepsilon_{DESIGN}$$

However, for the final baseline design, w_B was minimized when the tubing wall thickness, $r_o - r_i$, was the minimum practical size, 0.127 mm (0.005 inch).

Regarding effects of γ, the direction of the overall waviness, auxilliary calculations were performed on typical designs to determine the value of γ which would minimize p^*_{MAX}. Figure 4 shows the relationship between p^*_{MAX} and γ calculated during computations for the final baseline design. It is shown in Figure 4 that p^*_{MAX} is minimized at $\gamma \approx 60°$. Therefore, that value of γ was used throughout

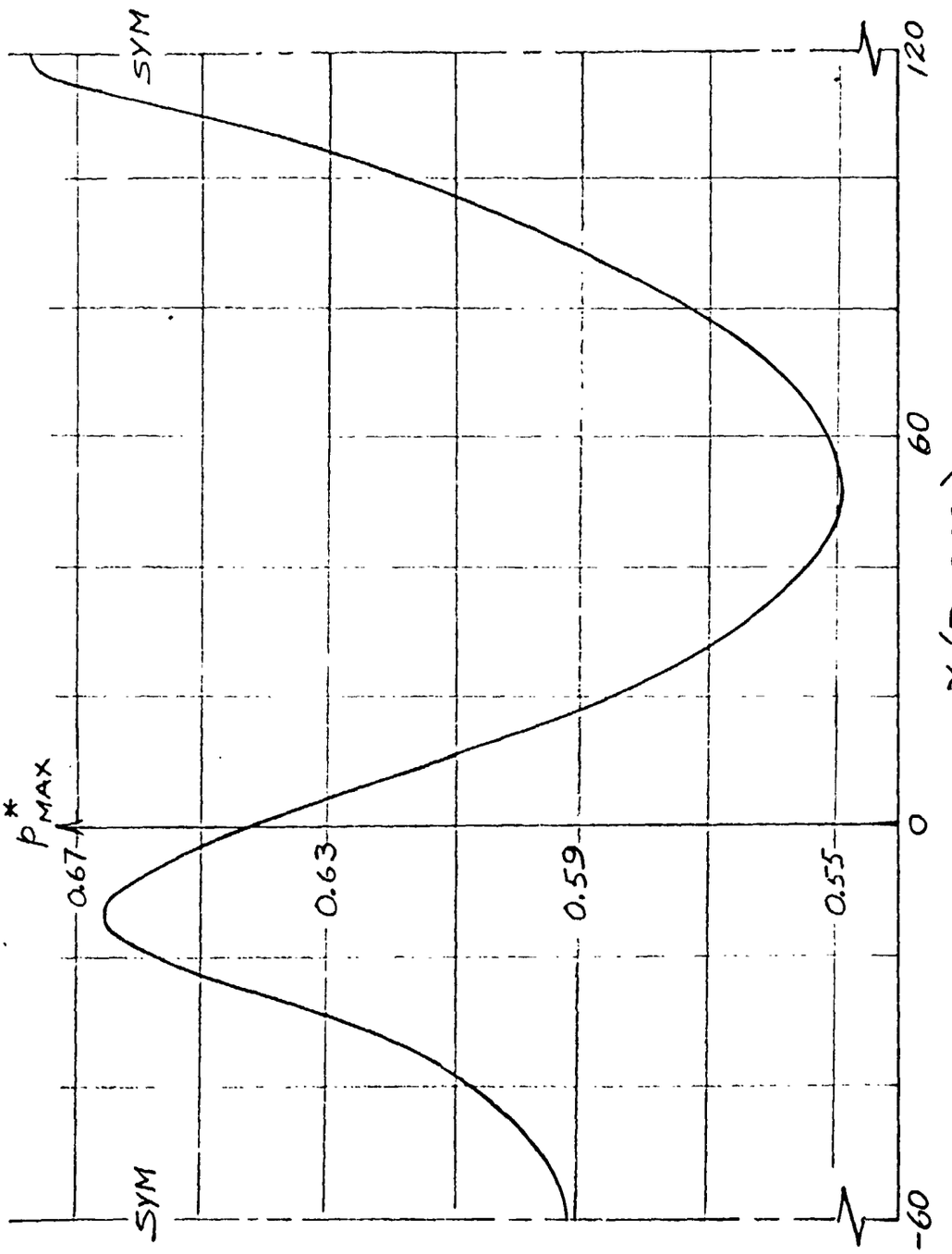

FIGURE 4 -- p^*_{MAX} Versus Angle γ of Initial Waviness

the investigation of the final design.

Sensitivity studies were performed to determine changes in w_B that would result from small changes in the various design variables. The method for computing such changes in w_B was simply to vary the input values of the variables and use the above-outlined computational procedures.

The results obtained by the above procedures are presented in the following section of this report.

CONCEPTUAL DESIGN DATA

Data are presented in this section, first on booms of several different materials which satisfy the Initial Design Criteria and Specifications. Then, data are presented on titanium booms which satisfy the Final Design Criteria and Specification. Finally, results of sensitivity analyses are presented which define boom mass changes that occur due to small changes in the various design variables.

Initial Conceptual Designs

Table 2 lists data on conceptual boom designs, for the six materials listed in Table 1, which designs were sized to satisfy the Initial Design Criteria and Specifications. Table 2 shows that the designs using Ti-6Al-4V and HTS-Graphite/Polyimide materials are the two least masssive. The other feasible designs (of steel, aluminum and S-Glass/Polyimide) are so much more massive that they were not considered further in this investigation. As noted on Table 2, the design strain for HM (high modulus) Graphite/Polyimide was too small for it to result in a feasible design. That is, for a boom of suitable strength to be made of that material would require that either the design strain be exceeded or that its diameter exceed the maximum specified diameter.

Table 2: Data on Conceptual Designs of Booms
Satisfying Initial Criteria and Specifications

Material	Boom Diam. (m)	Longeron Coiling Strain	Boom Mass (kg/m)	Comments
Ti-6Al-4V	1.168	0.00660	0.3095	Feasible & least mass
Steel	1.168	0.0043	0.6634	Too massive
7075-T6 Alum.	1.168	0.0058	0.5510	Too massive
HTS-Graph/Poly	0.800	0.0050	0.3101	Feasible & low mass
HM-Graph/Poly	---	----	----	ε_{DESIGN} too small for feasible design
S-glass/Poly	0.914	0.0062	0.5369	Too massive

Table 3 gives additional properties of the two most feasible designs, one of Ti-6Al-4V and the other of HTS Graphite/Polyimide. Most of the properties listed in Table 3 are self-explanatory and are in accordance with the previously presented Initial Design Criteria and Specification and Strength and Design Analysis. However, the following comments are given regarding the last three entries in Table 3.

1) Retracted length, H_B : This length is calculated as

$$H_B = \frac{3L}{2\pi R} (d_\ell + 0.00203) \text{ (meters)}$$

where the symbols are defined in Table 3. The 0.00203-term is the thickness (in meters) of the part of the longeron-to-batten fitting which prevents the coiled longeron members from lying against themselves. This interference thickness is determined from prior experience with fabricated booms.

2) Canister length, H_C ; The length required for a canister that can stow and deploy one spar is

$$H_C = 5H_B + 3R$$

This semi-empirical formula is based on the observations that a length of $5H_B$ is required to stow one coiled spar-length and a length of $3R$ is required to accomodate a deployment mechanism plus the boom transition length from its fully-coiled to its full-deployed configurations (see Figure 2).

3) Self-deployment force : This force has been derived by ABLE (see attached brochure) as

$$F = \frac{1.5EI_\ell}{R^2}$$

Table 3: Properties of Titanium and Graphite-Composite Booms - Initial Designs

Property	Titanium Boom	Graphite Boom
Material designation	Ti-6Al-4V	HTS-Graphite/Polyimide
Design axial strength, P(N)	137.9	137.9
Free-span length, L(m)	115.5	115.5
Total boom length in spacecraft, 23L(m)	2656.1	2656.1
Boom mass per unit length, w_B(kg)	0.3095	0.3101
Boom mass per L, W_B(kg)	35.75	35.82
Boom mass per spacecraft (kg)	822.06	823.66
Boom radius, R (m)	0.584	0.400
Longeron cross-section	Circular tube	Solid square
Longeron diameter(width), d_ℓ(cm)	0.772	0.401
Longeron wall thickness (cm)	0.028	----
Longeron coiling strain	0.0066	0.0050
Longeron coiling stress (N/m^2)	7.28×10^8	6.7×10^8
Retracted length for L, H_B(m)	0.921	0.833
Canister length for one spar, H_C(m)	6.357	5.364
Self-deployment force, F(N)	11.50	27.07

where EI_ℓ = bending stiffness of one longeron.

It is noted regarding the masses shown in Table 3 that detailed design studies were made of the titanium and graphite booms. Total masses for the two types of booms were derived from those design studies, which indicated that the weight-model used to analytically derived their masses was accurate within a few percent for predicting overall boom weight.

Final Conceptual Design

As noted earlier, titanium (Ti-6Al-4V) was selected to be the baseline material for the final conceptual design of the spars and mast. It was sized to satisfy the final design criteria and specifications. Axial loads and free-span lengths for the spars and masts were selected interactively and iteratively by JPL and ABLE. JPL calculated initial masses, loads and free-span lengths for the spar by estimating that for all its free-spans, the product PL^2 would be constant. ABLE then calculated the seven free-span lengths and section characteristics which could just withstand the specified loads (including appropriate inplane-stay-induced loads), yet have identical cross-sections and a constant total spar length. Mast free-spans were sized so that they had the same overall radius as the spars. But, their longeron cross-sections could differ from those of the spars, both in the two sunward (foreward) and in the two aft free-spans of the mast. JPL

then recalculated the axial loads for the new lengths and masses. After approximately four such iterative calculations, the lengths and axial loads for the spar and mast free-spans converged to the values listed in Table 4. Also listed in Table 4 are the bending stiffnesses that were calculated for each free-span when subjected to its respective design load. Note that those bending stiffnesses indicate "buckling" strengths that are significantly greater than the design axial loads. However, those buckling strengths cannot be realized.

It is noted that the loads listed in Table 4 are "design-values" for the longer spans (651.77 m), and that they are significantly less than the initial design loads for the shorter spans. It is also emphasized that the longeron wall thickness could be no less than 0.127 mm (0.005 inch). This latter specification along with the smaller axial loads and generally shorter free-spans led to spar-longeron designs whose optimum strains were less than the design limit strain listed in Table 1 for Ti-6Al-4V. However, the optimum overall diameters for spars and mast are the limit value, 1.168 m.

Table 5 lists mass, dimensional and mechanical properties of the spans for this final design, and Table 6 lists the same properties for each of the mast free-spans.

ABLE Drawings, numbered 460010 through 460020, which were delivered separately to JPL, give the results of a detailed design study of the spans. The following mass-breakdown for

Table 4: Axial Loads, Freespan Lengths and Bending Stiffnesses for Titanium Spar and Mast Designs

Boom No.	Axial Load/JPL (N)	Added* Load/ABLE (N)	Total Axial Load (N)	Free-span Length (m)	Bending Stiffness x 10^{-5} (N-m^2)
Spar					
1 (outer)	47.92	1.48	49.40	124.34	1.29
2	54.30	3.31	57.61	111.00	1.23
3	59.76	5.56	65.32	97.68	1.20
4	64.22	8.80	73.02	86.95	1.14
5	67.64	10.10	77.74	80.72	1.08
6	69.48	11.08	80.56	77.18	1.09
7	71.45	11.57	83.02	73.90	1.08
Mast					
1 (Fore)	19.88	---	19.88	88.26	0.545
2	19.60	---	19.60	94.43	0.545
3 (Aft)	97.54	---	97.54	94.04	1.55
4	91.91	---	91.91	96.88	1.55

* Axial load induced by inplane stays, calculated by ABLE

Table 5: Mass, Dimensional and Mechanical Properties of Final Titanium Spar Design

Total spar length	651.77 m
Spar mass per unit length	0.1781 kg/m
Mass of one spar	116.1 kg
Mass of four spars	464.4 kg
Spar diameter	1.168 m
Longerons; Ti-6Al-4V tubing, diameter and wall thickness	0.711cm x 0.0127cm
Battens; Ti-6Al-4V tubing, diameter and wall thickness	0.584cm x 0.0127cm
Longeron coiling strain	0.00609
Longeron coiling stress at R.T.	6.78×10^8 N/m^2
Retracted length per spar	4.33 m
Canister length for one spar	6.08 m
Ideal bending stiffness (for no waviness)	1.478×10^5 N-m^2
Actual bending stiffness	(see Table 4)
Ultimate bending strength (min)	44.9 N-m
Shearing stiffness	3×10^4N
Torsional stiffness	0.510×10^4 N-m^2
Torsional strength	8.40 N-m
Diagonal pretension	4.14 N

Table 6: Masses, Dimensions and Properties of Final Titanium Mast Designs*

Property	Mast Number			
	1	2	3	4
Free-span length (m)	88.26	94.43	94.04	96.88
Mass of free-span (kg)	12.47	13.34	18.81	19.37
Longeron (Ti-6Al-4V) Diameter (cm)	0.452	0.452	0.777	0.777
Wall thickness (cm)	0.0127	0.0127	0.0178	0.0178
Batten (Ti-6Al-4V) Diameter (cm)	0.356	0.356	0.635	0.635
Wall Thickness (cm)	0.0127	0.0127	0.0178	0.0178
Longeron coiling strain	0.00387	0.00387	0.0066	0.0066
Longeron coiling stress at R.T. (N/m^2)	4.27×10^8	4.27×10^8	7.28×10^8	7.28×10^8
Retracted length (m)	0.399	0.427	0.675	0.696
Bending stiffness ($N-m^2$)	0.545×10^5	0.545×10^5	1.55×10^5	1.55×10^5
Ultimate bending strength (N-m)	11.09	11.09	58.43	58.43

*Overall diameter, baylength, diagonal construction, shearing stiffness, shearing strength and diagonal pretension same as for spars; see Table 5

one spar was determined from the detailed design.

Part	Mass (kg)
Longerons	24.17
Battens	32.79
Corner fittings	40.27
Diagonals	18.59
Adhesive	0.28
Total	116.10

Detailed drawings were not made of the final design of the mast.

Mass Sensitivities of Final Spar Design

Figure 5 shows normalized mass changes of the middle free-span of the final spar design, that were calculated to result from ±10% changes in the design variables L, P, n, y_ℓ/ℓ, y_L/L and R . It is evident from Figure 5 that the mass is highly sensitive to changes in both P and L . Therefore, it was important to accurately define and calculate those variables in the previously discussed iterative design analysis.

Small changes in the waviness parameters y_ℓ/ℓ and y_L/L are shown in Figure 5 to have only small influence on spar mass. However, that trend should not be extrapolated too far regarding reductions in waviness. That is, as shown by Figure C4 of Appendix C, the compressive strength of a lattice boom is greatly decreased from its ideally-straight

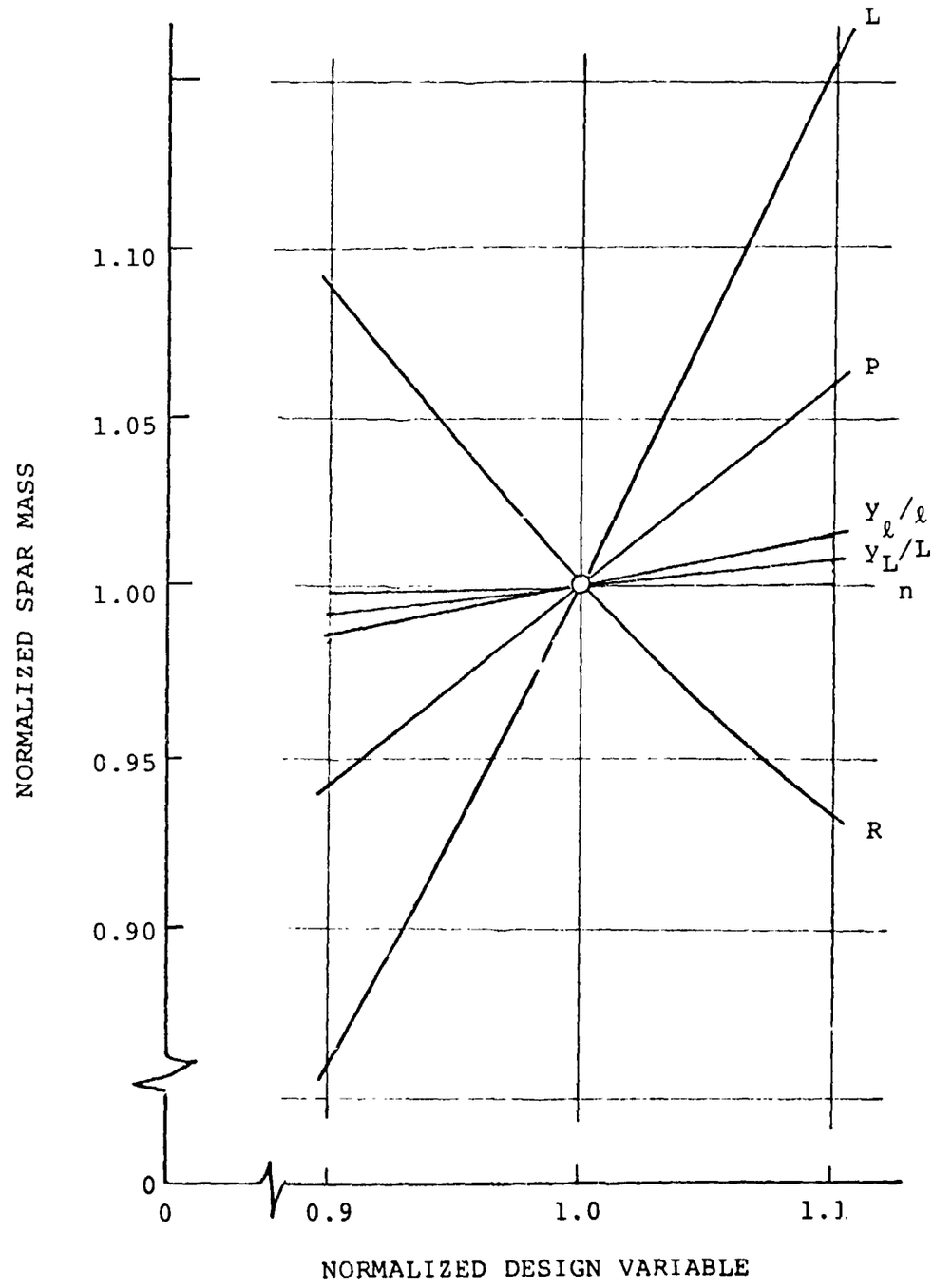

FIGURE 5 -- Sensitivity of Spar Mass to Changes in Design Variables; Typical for Spar Middle Free-span

strength by introducing only a small amount of initial waviness. As such initial waviness increases, the strength reduction decreases. Thus, the insensitivity to changes in y_ℓ/ℓ and y_L/L shown by Figure 5 is valid only for small deviation from the specified values of those parameters.

Figure 6 shows the influence of the ratio of baylength-to-radius, ℓ/R, on spar mass. It is clear from Figure 6 that the selection of $\ell/R = 1.0$ did not result in minimum spar mass. Minimum mass is obtained at $\ell/R = 1.15$, which is the intersection of designs governed by longeron minimum wall thickness with those that are strain-limited. However, $\ell/R = 1.0$ was selected because it provides for a shorter retracted length for the spar than would a design for which $\ell/R = 1.15$. This shorter retracted length was necessary to satisfy a dimensional limit on the stowage envelope, which limitation was emphasized late in this investigation.

A study was also made of the spar mass changes that would result from changing its number of freespans to six or eight. The resulting spar masses are listed below, along with the corresponding longeron diameters and retracted lengths of the spars.

No. of Freespans	Spar Mass (kg)	Longeron Diameter (cm)	Retracted Spar Length (m)
6	119.9	0.765	4.62
7	116.1	0.772	4.33
8	111.9	0.653	4.01

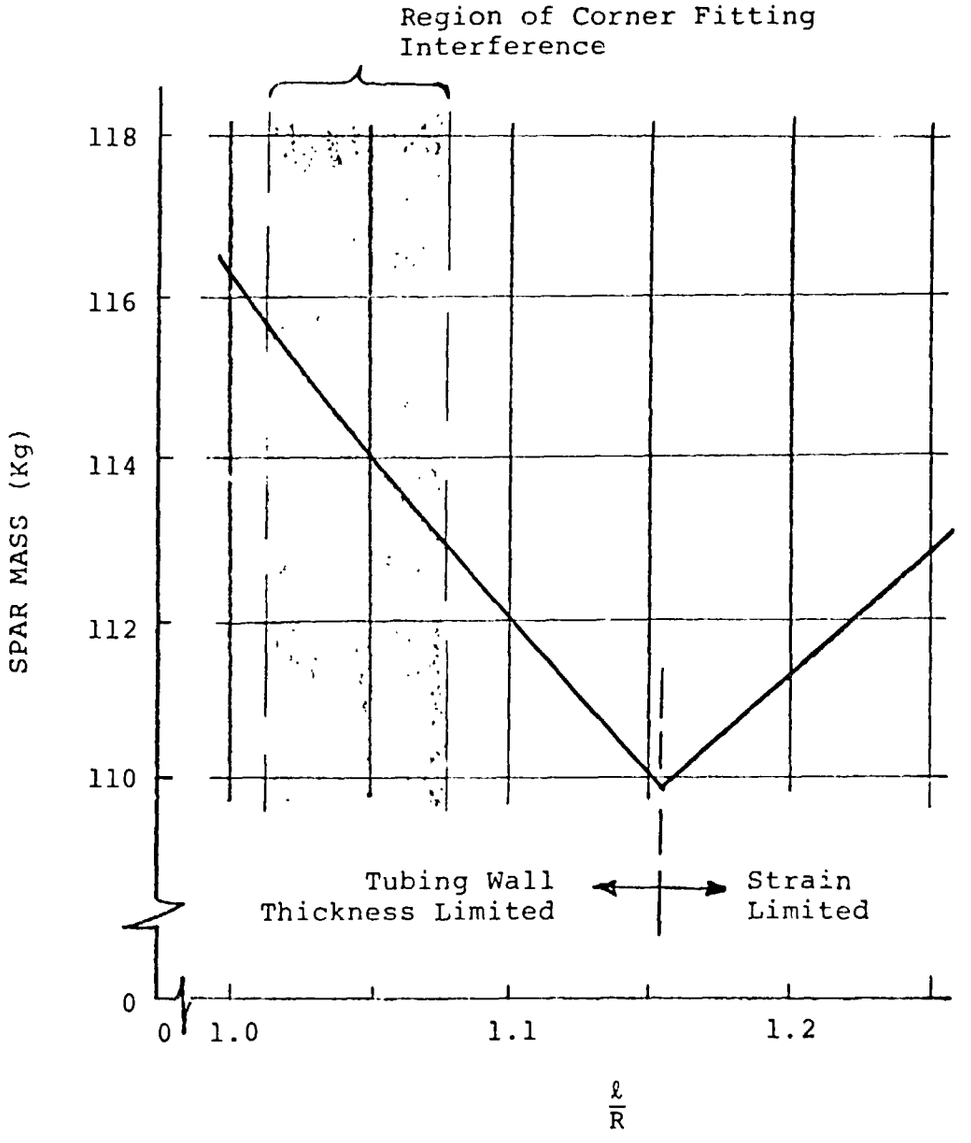

FIGURE 6 -- Spar Mass Variation with Ratio of Baylength-to-Boom Radius; Final Titanium Design

It is evident from these data that the resulting mass changes are small; about ±3% . However, the available stowage length did not permit the option of using six free-spans. Although the selection of eight free-spans would have further decreased the retracted length and mass, it would also increase system complexity and ancillary mass. Therefore, the selection of seven free-spans for the spar appears to be optimum for the overall system.

CONCLUSIONS

This investigation resulted in the conceptual design of deployable titanium lattice booms to function as the four spars and central mast of a Solar Sailer spacecraft. The total mass of the four spars and central mast is 528.4 Kg, or about 0.73 g/m^2 for the 850-m square sail area.

The conceptual design appears to be feasible inasmuch as it was designed in compliance with a comprehensive strength analysis and well established technology which has been used on prior designs of deployable lattice booms having S-glass/epoxy and S-glass/polyide longeron and batten members. In fact, as an adjunct to this investigation, thin-walled steel tubing was subjected to bending and twisting deformations similar to those that the titanium tubing would experience in this application. The steel tubing withstood the deformations, proving that longerons of deployable lattice booms can be made of metallic tubing.

However, technology still needs to be developed for these booms in the following areas:

1) Drawing or chemical milling of titanium tubing to realize the required, thin wall-thicknesses.

2) Processes and tooling for making well-aligned joints between segments of longeron tubing and boom assemblies; using metallurgical or adhesive bonds, or mechanical fasteners.

3) Design of diagonal members of booms to survive micrometeoroid threat.

4) Statistical prediction of initial waviness of longerons and overall-boom assembly, plus design methods which account for such waviness statistics.

5) Methods for measuring initial waviness in long boom assemblies, which account for gravitational deformations.

Note that most of these areas are associated with developing technology to detect, minimize, predict and design-for effects of waviness in the longerons and the boom assemblies. Development of this technology is necessary because of the very significant effects that such waviness was shown to have on the present conceptual design.

Appendix A

INITIAL WAVINESS ESTIMATES FOR LONGERONS AND THE OVERALL BOOMS

This appendix presents estimates that were made of the initial wavinesses of both the longerons and the overall boom assemblies. Longeron wavinesses, as they were estimated to arise from several different sources, are presented first. Subsequently, overall boom waviness estimates are presented. These estimates are the basis for the selected design values of the waviness parameters;

$$y_\ell/\ell = \frac{1}{2500}$$

and

$$y_L/L = \frac{1}{1000}$$

Longeron Initial Waviness

The initial waviness of each longeron in each baylength of the spars and masts is assumed to be the sum of geometrically similar wavinesses which arise from several different sources. Following are estimates of waviness amplitudes for all of the sources that were considered to be significant.

Curvature of Longeron Stock -- It is assumed that the longeron tubing is precurved to a constant radius ρ . This radius

can be calculated from the straightness specification which the supplier will meet,

$$\rho = \frac{\ell_o^2}{8y_o}$$

where y_o is the specified wave amplitude in a specified length ℓ_o. An initial waviness can result from using such stock tubing because the ends of the longerons in the terminal baylengths of each segment of a spar assembly will have that initial curvature. This condition is as shown below.

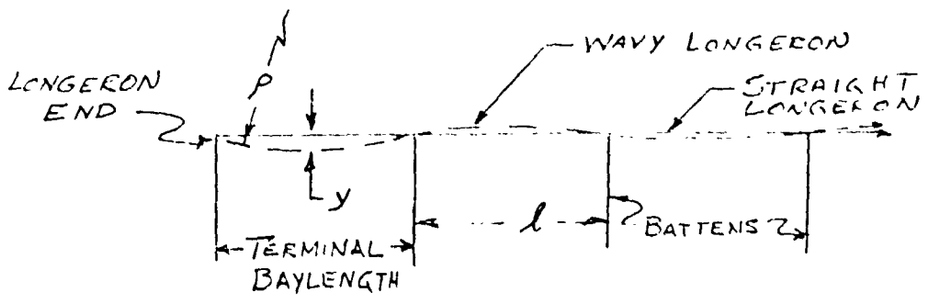

For this condition, the maximum deflection y is that for the series of simply supported beams acted upon at its end by a moment M which would give the prescribed curvature at the end, for which

$$y = 0.048 \frac{M\ell^2}{EI}$$

Since

$$\frac{1}{\rho} = \frac{M}{EI}$$

$$y = 0.048 \frac{\ell^2}{\rho}$$

By using the previously given expression for ρ, the maximum deflection becomes

$$y = 0.384\ y_o\left(\frac{\ell}{\ell_o}\right)^2$$

The ASME standard for acceptably straight tubing is 0.010 inches of bow in any 12 inches of length. For tubing to just meet the ASME standard and for that tubing to be selected and used in the boom assembly is estimated to be a 4σ occurrence. Therefore, the 1σ initial bow is estimated to be $y_o = 0.0025$ inch for $\ell_o = 12$ inches. Accordingly, for the 23-inch baylength,

$$y = 0.384\ (0.0025)\left(\frac{23}{12}\right)^2$$

$$= 0.00353 \text{ inch}$$

Temperature Difference Across Longerons -- A linear temperature gradient of $\Delta T/2r$ across an unrestrained longeron will cause it to curve to a radius ρ given by

$$\rho = \frac{2r}{a\Delta T}$$

where r = longeron radius

and a = longeron coefficient of linear thermal expansion

When this temperature gradient is discontinuous over a longeron length or when a longeron terminates, the deflection of the longeron in the adjacent baylength is, as in the previous analysis,

$$y = 0.048\ \frac{\ell^2}{\rho}$$

or $$y = 0.024 \frac{a\Delta T \ell^2}{r}$$

For a titanium longeron of the baseline design

$$a = 5 \times 10^{-6}/°F$$

$$r = 0.140 \text{ inch}$$

$$\ell = 23 \text{ inches}$$

Although the temperature difference ΔT across a directly irradiated, thin-walled titanium longeron could be approximately 40°R at 0.3 AU, it is estimated that when irradiated only diffusely by the sail, then

$$\Delta T \simeq 5°R$$

For which, the foregoing formula gives

$$y = 0.00227 \text{ inches}$$

This waviness would develop only during operation of the spacecraft. Therefore, it would exist only in outboard baylengths of spars. However, for conservatism, it is included here as though it could occur over the lengths of the spars.

Differences Among Diagonal Lengths -- The lengths of the diagonal members of a boom can differ for various reasons, including dimensional tolerances in their manufacture, dimensional tolerances in their retainers, and temperature differences among the diagonals. In any event, such differences will cause twisting and/or shearing of the boom. And, localized twisting and shearing will cause the longerons of the boom to bend; thus, have an initial waviness.

The following sketch shows a longeron (free to rotate at ends) in a baylength that is sheared or twisted relative to longerons in adjacent undistorted baylengths.

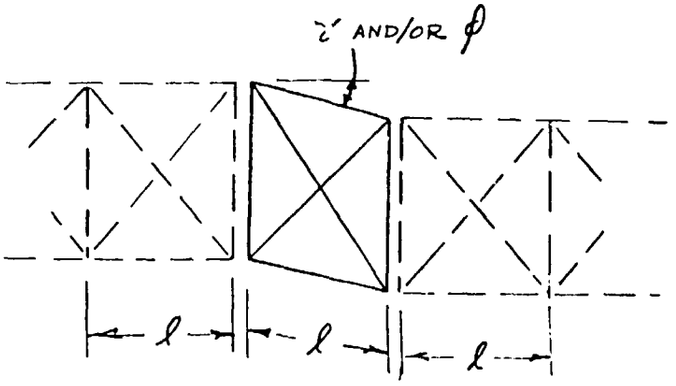

For the adjacent longeron segmerts to be continuous with the longerons in the distorted baylength requires that they have the same slope at their juncture instead of the indicated slope-discontinuity. Therefore, at the junctures bending moments M will exist in the longerons to enforce the slope continuity. The bending moment is calculated as indicated below.

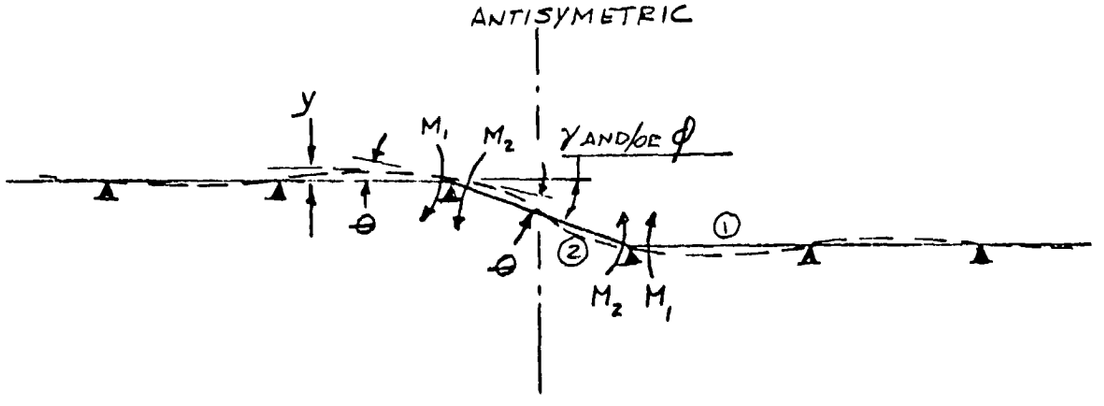

For equilibrium,

$$M_1 = M_2 = M = K_1\theta = K_2\ (\gamma - \theta)$$

Therefore,
$$\theta = \frac{\gamma}{1 + \frac{K_1}{K_2}}$$

or
$$M = \frac{K_1\gamma}{1 + \frac{K_1}{K_2}}$$

For beam (1), $K_1 = \frac{M}{\theta} = 3.46\ \frac{EI}{\ell}$

and, for beam (2), $K_2 = \frac{M}{\theta} = \frac{6EI}{\ell}$

Since the maximum deflection in beam (1) is

$$y = 0.048\ \frac{M\ell^2}{EI}$$

then
$$y = 0.1053\ \gamma\ell$$

and/or
$$y = 0.1053\ \phi\ell$$

From NASA CR-112183, "Development of a Microwave Inteferometer Position Locator", it is determined that the twist ϕ and shear γ of a baylength of this presently considered type of lattice boom are

$$\phi = \frac{\Delta_{1R} - \Delta_{1L} + \Delta_{2R} - \Delta_{2L} + \Delta_{3R} - \Delta_{3L}}{3R\cos\beta}$$

$$\gamma = \frac{2}{3}\sqrt{\gamma_1^2 + \gamma_2^2 + \gamma_3^2 - \gamma_1\gamma_2 - \gamma_2\gamma_3 - \gamma_1\gamma_3}$$

where $\gamma_1 = \frac{\Delta_{1R} - \Delta_{1L}}{2\ell \cos \beta}$

$\gamma_2 = \frac{\Delta_{2R} - \Delta_{2L}}{2\ell \cos \beta}$

$\gamma_3 = \frac{\Delta_{3R} - \Delta_{3L}}{2\ell \cos \beta}$

Δ_{iR} = diagonal length deviation in an i^{th} panel (i = 1, 2 or 3) of a baylength, which diagonal spirals in the right-hand (R) direction.

Δ_{iL} = length deviation in lefthand spiralling (L) direction of i^{th} panel

ℓ = longeron length

R = boom radius

β = Angle between batten and diagonal
= 30° for present design

For example, if Δ_o is the specified tolerance for the diagonal lengths, and if in one baylength all $\Delta_i = \Delta_o$ and all Δ_i have the appropriate sign to maximize ϕ and γ, then

$$\phi = \frac{2\Delta_o}{R \cos \phi} \quad \text{and} \quad \gamma = \frac{2\sqrt{6}\,\Delta_o}{3\ell \cos \phi}$$

Or, if in a baylength only one diagonal has the maximum tolerance and the others are perfect,

$$\phi = \frac{\Delta_o}{3R \cos \beta} \quad \text{and} \quad \gamma = \frac{\Delta_o}{3\ell \cos \beta}$$

By an approximate evaluation of the gamut of possible combinations of tolerances that can occur and their respective probabilities, plus consideration that ϕ and γ can be additive, it is estimated that a probable (1σ) distortion is

$$\phi + \gamma = \frac{2\Delta_o}{R \cos \beta}$$

(Note $\ell = R$ for this design)

Accordingly,

$$y = 0.2432\Delta_o$$

From previous manufacturing experience, it is estimated that $\Delta_o = 0.010$ inches will be achievable as a 1σ tolerance. Therefore,

$$y = 0.00243 \text{ inch}$$

Splice Misalignment -- It is considered here that tooling used to join longeron segments can enforce some misalignment in those joints, as indicated below by θ_o

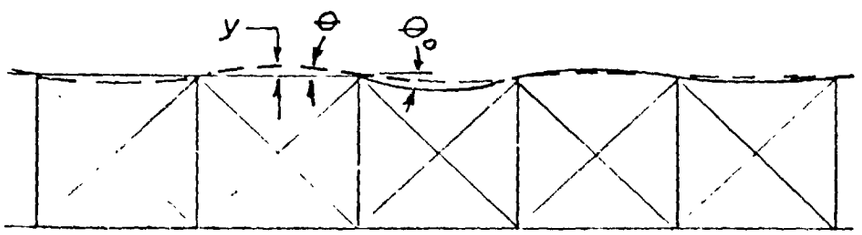

Upon releasing the tooling, such a misaligned longeron joint will rotate to the equilibrium position indicated, where

$$\theta = \frac{1}{2}\theta_o$$

The internal bending moment at the joint will then be

$$M = 3.46 \frac{EI\theta}{\ell} = \frac{1.73\ EI\theta_o}{\ell}$$

and the associated maximum deflection is

$$y = 0.048 \frac{M\ell^2}{EI}$$

$$= 0.08304\ \theta_o \ell$$

It is estimated that in production θ_o will be at least one milliradian. Therefore,

$$y = 0.08304\ (0.001)\ (23)$$

$$= 0.00191 \text{ inch}$$

Several other sources of longeron waviness were examined, but they were all found to be negligible compared to the foregoing.

Summary of Longeron Waviness -- The sum of the foregoing longeron initial wavinesses is

$$y = 0.01014 \text{ inch}$$

Consistently,

$$\frac{y_\ell}{\ell} = \frac{1}{2268}$$

However, the following reduced value of the waviness parameter is used in the text of this report:

$$\frac{y_\ell}{\ell} = \frac{1}{2500}$$

Overall Boom Initial Waviness

The initial overall waviness of each free-span of the spars and mast are assumed to be the sum of contributing wavinesses that arise from several different sources. Following are estimates of waviness amplitudes for all such sources that were found to be significant.

Splice Misalignment -- It is considered that when boom segments are spliced, either gaps between butting longerons or unequal-length longerons can cause splice misalignment, as indicated below.

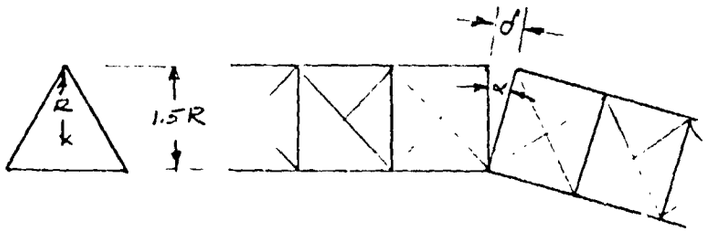

Here, δ is either the gap dimension or the longeron length inequality. The angular misalignment α that occurs owing to δ is

$$\alpha = \frac{\delta}{1.5\ R}$$

Since these individual misalignments can occur in random directions, the cumulative misalignment $\bar{\alpha}$ from joining $N + 1$ segments (N joints) to assemble a free-span length L is estimated from random-walk theory for a 1σ occurrence as

$$\bar{\alpha} = \sqrt{N}\ \alpha$$

$$= \frac{2\delta\ \sqrt{N}}{3R}$$

The average radius of curvature $\bar{\rho}$ for the span is then

$$\bar{\rho} = \frac{L}{\bar{\alpha}}$$

And, the resulting wave amplitude for the span is

$$y = \frac{L^2}{8\bar{\rho}}$$

$$= \frac{L\delta\ \sqrt{N}}{12R}$$

A 1σ gap is estimated to be

$$\delta = 0.015 \text{ inch}$$

Maximum available lengths of longeron tubing is reported by suppliers to be approximately 240 inches. Lengths of the outboard, middle and root spans of the spars for the Solar Sailer are, respectively,

$$L_1 = 4895 \text{ inches}$$

$$L_4 = 3423 \text{ inches}$$

and $$L_7 = 2910 \text{ inches}$$

Therefore, the waviness amplitude in each owing to gaps of 0.015 inch are

$$y_1 = \frac{4895\ (0.015)\ \sqrt{20}}{12\ (23)}$$

$$= 1.190 \text{ inches}$$

$$y_4 = \frac{3423\ (0.015)\ \sqrt{14}}{12\ (23)}$$

$$= 0.696 \text{ inches}$$

and

$$y_7 = \frac{2910\ (0.015)\ \sqrt{12}}{12\ (23)}$$

$$= 0.548 \text{ inch}$$

A 1σ length deviation between either one short longeron and two long ones, or one long longeron and two short ones, is estimated to be

$$\delta = 0.020 \text{ inch}$$

According to the same formula, the waviness amplitude in the three spans owing to this longeron length deviation is then

$$y_1 = 1.587 \text{ inches}$$

$$y_2 = 0.928 \text{ inch}$$

$$y_3 = 0.731 \text{ inch}$$

Temperature Differences Between Longerons -- Appendix B shows that a slight temperature difference can occur between the sailward and outward longerons of an outboard free-span of a spar. That temperature difference was shown to cause a difference in those longeron lengths of

$$\Delta L = 6.88\ aT_S$$

where T_S = sail temperature

and a = longeron coefficient of linear thermal expansion

This ΔL will cause the free-span to have a radius of curvature ρ given by

$$\rho = \frac{1.5\ RL}{\Delta L}$$

$$= \frac{1.5\ RL}{6.88\ aT_S}$$

and, since the waviness amplitude is given by

$$y_1 = \frac{L^2}{8\rho}$$

then

$$y_1 = \frac{0.573\ LaT_S}{R}$$

For $L_1 = 4895$ inches

$a = 5 \times 10^{-6}/°R$

$T_S = 980°R$

and $R = 23$ inches

$$y_1 = 0.598 \text{ inch}$$

The inboard free-spans of the spars should have virtually no temperature differences among their longerons; therefore, no waviness owing to this effect.

Differences Among Diagonal Lengths -- The "Longeron" section of this appendix gives a formula for the shear γ of a baylength of a boom in terms of deviations Δ in the lengths of the diagonals. With reference to that formula, it is assumed here that four of the six diagonals in a baylength have equal deviations Δ_o of the necessary signs to produce pure shearing of that baylength.

Then, the formula gives the shear angle

$$\gamma = \frac{2\Delta_O}{\sqrt{3}\ \ell \cos \beta} \qquad (\beta = 30°)$$

(see previously given definition of symbols)

Therefore, the shear deflection per baylength, y_i, is

$$y_i = \gamma \ell$$

$$= \frac{4\Delta_O}{3}$$

It is now considered that the deflection owing to random-walk effects for N baylengths in one-half a free-span length is (for 1σ occurrence)

$$y = \sqrt{N}\ y_i$$

$$= \frac{4\Delta_O\ \sqrt{N}}{3}$$

It is implicit in this formula that the other half of the free-span is oppositely but equally sheared. That probability is accounted for by using one-half y given by the above formula to estimate the deflection due to this effect. Note also that

$$N \simeq \frac{L}{2\ell}$$

It is estimated (as before) that $\Delta_O = 0.010$ inch is a 1σ occurrence. Then, the wave amplitudes for the outboard, middle and root free-spans of a spar are, respectively,

$$y_1 = \frac{2\ (0.010)}{5} \sqrt{\frac{4895}{2\ (23)}}$$

$$= 0.069 \text{ inch}$$

and similarly $y_2 = 0.057$ inch

$y_3 = 0.053$ inch

External Forces -- Aside from the lateral acceleration forces which are accounted for in the text of this report, only the outboard free-spans of the spars are subjected to forces which can cause initial deflection. Owing to attached control surfaces, the outboard end of the spars are subjected to shears and bending moments. The effect of the shearing force is neglected here since it is carried mostly by the outboard stay. However, the bending moment, which is estimated by JPL to be about 50 in-lb, is considered. The maximum deflection that is produced by this bending moment is calculated from the previously given formula for deflection of a beam over many simple supports as,

$$y = 0.048 \frac{ML^2}{EI}$$

For the outboard free-spans,

$L = 4895$ in

$EI = 4.49 \times 10^7$ lb-in^2 (See text)

and $M = 50$ in-lb

Then, $y = 1.28$ inches

Temperature Difference Across Longerons -- As noted previously in this appendix, a linear temperature gradient $\Delta T/2r$ across an unrestrained longeron will cause it to curve to a radius

$$\rho = \frac{2r}{a\Delta T}$$

The boom will, however, resist taking on that curvature. In fact, the boom will bend only in response to an internal bending moment M which is necessary to approximately straighten the three individual longerons. That is

$$M = 3M_\ell$$

where

$$M_\ell = EI_\ell \left(\frac{1}{\rho} - \frac{1}{\rho_B}\right)$$

EI_ℓ = longeron bending stiffness

ρ_B = radius to which the overall boom curves in its reaction

Since

$$M = \frac{EI_B}{\rho_B}$$

where EI_B = boom bending stiffness

then

$$\frac{EI_B}{\rho_B} = 3EI_\ell \left(\frac{1}{\rho} - \frac{1}{\rho_B}\right)$$

or,

$$\frac{1}{\rho_B} = \frac{1}{\rho}\left(\frac{1}{1 + \frac{EI_B}{3EI_\ell}}\right)$$

The deflection at the midlength of a free-span is then

$$y = \frac{L^2}{8\rho_B}$$

$$= \frac{L^2}{8\rho}\,\frac{1}{1 + \frac{EI_B}{3EI_\ell}}$$

$$= \frac{L^2 a \Delta T}{16r} \frac{1}{1 + \left(\frac{R}{r}\right)^2}$$

For the outboard free-span,

$L_1 = 4895$ inches

$a = 5 \times 10^{-6}/°R$

$\Delta T = 5°R$

$r = 0.14$ inch

$R = 23$ inches

Therefore, $y_1 = 0.0099$ inch

Summary of Overall Boom Waviness -- The sum, y_L, of the foregoing overall wavinesses for the outboard, middle and root free-spans of a spar are listed below.

Span	L (in)	y_L (in)	$\left(\frac{y_L}{L}\right)^{-1}$
Outboard	4895	4.142	1182
Middle	3423	1.697	2017
Root	2910	1.348	2159

The value of y_L/L used in deriving the baseline design was

$$\frac{y_L}{L} = \frac{1}{1000}$$

Appendix B

BENDING DUE TO ΔT BETWEEN LONGERONS

The objective of this analysis is to calculate the thermal bending that will occur in the diagonal spars because of temperature differences between longerons nearer to and farther from the sail. These temperature differences are anticipated to be most severe at the outboard end of the spars where the longeron nearer the sail has a much larger view factor of the sail than does the farther longeron, as indicated below.

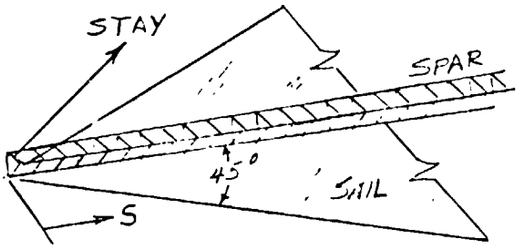

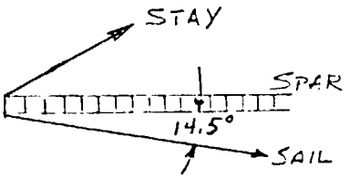

View factors at stations along each longeron were estimated by assuming the sail width (perpendicular to longeron) is finite, but the length (parallel to longeron) is infinite. The sail was assumed to be planar and to extend at an angle of 14.5° to the longerons, with the sail apex coincident with the outboard end of the sailward longeron. The view factors were calculated accordingly, using the formula given for "Condition 4" in the HANDBOOK OF HEAT TRANSFER, pages 15-44.

Temperatures along each longeron were calculated by assuming grey-body, steady-state conditions for the sail and longerons according to the following formula derived by the Poljak method:

$$\frac{T_\ell}{T_S} = \sqrt[4]{\frac{1}{1 + \frac{\alpha_\ell}{F_{S\ell}} \frac{A_\ell}{A_S} \left[1 + \left(\frac{1}{\alpha_S} - 1 \right) F_{S\ell} + \left(\frac{1}{\alpha_\ell} - 1 \right) F_{S\ell} \frac{A_S}{A_\ell} \right]}}$$

where T_ℓ = longeron temperature

T_S = sail temperature

α_ℓ = absorptivity of longeron

α_S = absorptivity of sail

$F_{S\ell}$ = view factor; sail to longeron

A_S = sail area (width per unit length)

A_ℓ = longeron area (surface area per unit length)

Figure B1 gives longeron-to-sail temperature ratios T_ℓ/T_S as they vary along the longerons for the conditions

$$\alpha_S = 0.55$$

$$\alpha_\ell = 0.22$$

and $$\frac{A_\ell}{A_S} = \frac{\pi d}{2L}$$

where $d = 0.304$ inch = longeron diameter

and S = half width of sail at a distance S from the sail apex

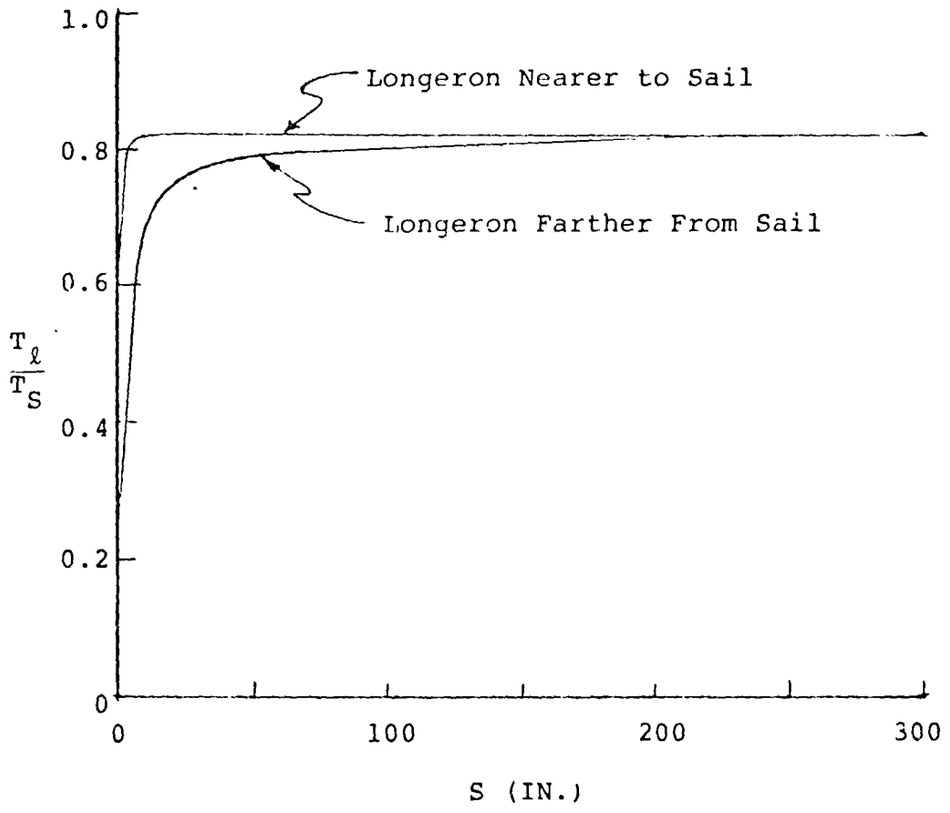

FIGURE B1 -- Longeron-to-Sail Temperature Ratio Along Nearer and Farther Longerons

It is evident from Figure B1 that no significant temperature difference exists between the nearer and farther longerons for distances greater than 220 inches from the sail apex.

The difference ΔS in thermal expansions between the nearer and farther longerons, over the length where the expansions are significant, is

$$\Delta S = aT_S \int_0^{220} \left(\frac{T_{\ell/N}}{T_S} - \frac{T_{\ell/F}}{T_S} \right) dS$$

where a = longeron coefficient of thermal expansion

$T_{\ell/N}$ = temperature of longeron nearer to sail

$T_{\ell/F}$ = temperature of longeron farther from sail

The integral in the above equation was determined from Figure B1 to be 6.88 inches. Therefore,

$$\Delta S = 6.88\ aT_S$$

For $T_S = 980°R$ and $a = 5 \times 10^{-6}/°R$ (for titanium),

$$S = 0.0337 \text{ inch}$$

If the outboard span of the boom is pin-jointed at a distance L from its end (see sketch below), then $\Delta S = \Delta L$ and it will cause that span to bend to a radius R_B given by

$$R_B = 1.5\ R\frac{L}{\Delta L}$$

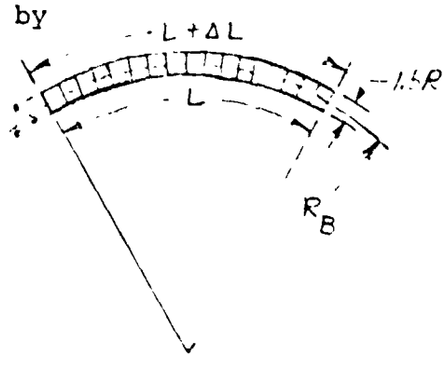

The resulting bow at the midspan of L is given approximated by

$$y_L = \frac{L^2}{8R_B}$$

Appendix C

STRENGTH OF A WAVY LATTICE COLUMN

Following are the principal assumptions made in this analysis:

1. The column is a three-sided lattice structure as shown in Figure C1, simply supported with spanlength L, baylength ℓ and radius R.

2. It is axially compressed by load P and laterally loaded by a uniformly distributed inertial load nW, where W is the weight of the column and n is a load factor.

3. The initial waviness of the axis of the column assembly is

$$y = y_L \sin \frac{\pi x}{L} \tag{C1}$$

and the initial waviness of all its longeron axes is

$$y = y_\ell \sin \frac{\pi x}{\ell} \tag{C2}$$

4. In reaction to P, the column axis deflects in the same mode as its initial waviness. (Note that for small deflections of a sinusoidally wavy column of uniform bending stiffness and simply supported, this mode of reaction is exact. However, it is only an approximation for a column of nonuniform bending stiffness and laterally loaded.)

5. The lattice column has a uniform bending stiffness along its length which is equal to the minimum stiffness that is calculated for its midlength.

6. The column is so oriented that in reaction to lateral inertial loading, two longerons are equally compressed while the third is tensioned.

7. The direction in which the column is initially wavy is that which produces minimum compressive strength (as derived herein).

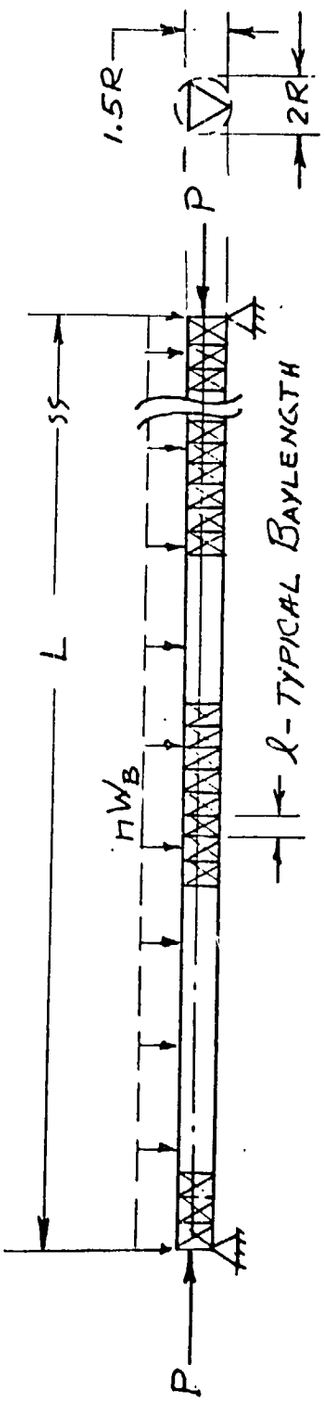

FIGURE C1 -- Simply Supported Lattice Column, Axially and Laterally Loaded

8. All stresses are elastic.

9. Effects of finite transverse shearing stiffness are negligible.

Consistent with the foregoing assumptions, the classical buckling strength P_B for this column is

$$P_B = \frac{\pi^2 EI_B}{L^2} \tag{C3}$$

where EI_B is the assumed uniform bending stiffness of the column. Because this initially wavy column will bend upon application of compression load P, as well as lateral load nW, its longerons will become unequally loaded. And, because the longerons themselves are initially wavy, they will exhibit unequal axial stiffnesses under their unequal loadings, as shown later in the analysis.

Without definitizing the longeron stiffnesses, the following formula for the bending stiffness of this column, with unequal longeron stiffnesses, was derived by direct application of statics and the usual assumption that sections of the column which are plane before bending remain plane after bending:

$$EI_B = \frac{3AER^2}{4}\left[\frac{\frac{E}{E_1}(\sin\gamma + \sqrt{3}\cos\gamma)^2 + \frac{E}{E_2}(\sin\gamma - \sqrt{3}\cos\gamma)^2 + \frac{E}{E_3}\,4\sin^2\gamma}{\frac{E}{E_1}\frac{E}{E_2} + \frac{E}{E_1}\frac{E}{E_3} + \frac{E}{E_2}\frac{E}{E_3}}\right] \tag{C4}$$

where A = longeron cross-sectional area, same for each longeron

E = Young's modulus of elasticity for longeron material

R = column radius; see Figure C1

γ = angle between neutral plane of bending and one face of the column; see Figure C2

E_i = effective Young's moduli for each of the three longerons; see Figure C2 for numbering convention

Axial forces F_i in the longerons are considered to be the sum of three sources,

$$F_i = F_i^P + F_i^y + F_i^W \quad (i = 1, 2 \text{ and } 3) \tag{C5}$$

where F_i^P = forces induced by P, for axial equilibrium of forces when column is straight

F_i^y = midlength forces necessary to equilibrate the bending moment produced by P and the initial column waviness

and F_1^W = midlength forces necessary to the bending moments produced by both P and deflections due to nW and by applied moments due to nW

For axial equilibrium between P and the longeron sections,

$$F_1^P = F_2^P = F_3^P = \frac{P}{3} \tag{C6}$$

At the column midlength, an internal bending moment M_γ will be necessary to equilibrate the externally applied moment owing to the load P acting at the eccentric distance y. The distance y is the total deflection of this initially wavy column in the direction of the initial waviness, and it is given by THEORY OF ELASTIC STABILITY, by S. Timoshenko, p. 32, as

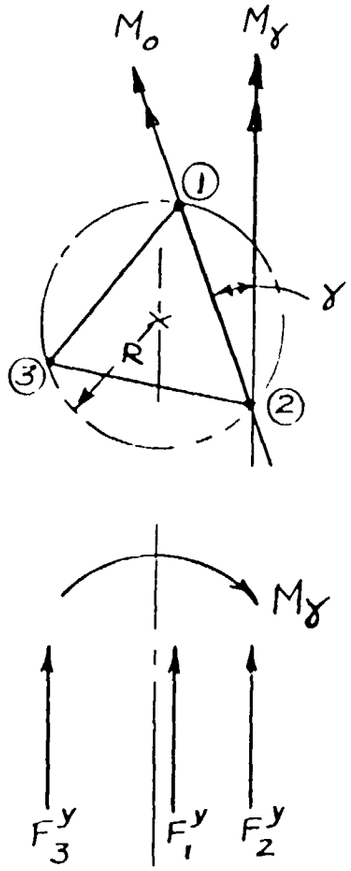

F_i^y = Longeron Forces, Positive in Compression

(1) = Longeron No. 1; Modulus = E_1

(2) = Longeron No. 2; Modulus = E_2

(3) = Longeron No. 3; Modulus = E_3

FIGURE C2 -- Moment and Reactive Longeron Forces on Column

$$y = \frac{y_L}{1 - p_B^*} \tag{C7}$$

where

$$p_B^* = \frac{P}{P_B} \tag{C8}$$

Accordingly, the internal bending moment M_γ is given by

$$M_\gamma = \frac{Py_L}{1 - p_B^*} \tag{C9}$$

Longeron axial loads F_i^y which provide M_γ are determined from statics as follows. For equilibrium in the direction of the column axis,

$$F_1^y + F_2^y + F_3^y = 0 \tag{C10}$$

for equilibrium of moments in the direction of M_γ (moments summed about longeron (2), see Figure C2),

$$F_1^y R\sqrt{3}\sin\gamma + F_3^y R\frac{\sqrt{3}}{2}(\sin\gamma + \sqrt{3}\cos\gamma) + M_\gamma = 0 \tag{C11}$$

And, because the sum of the moments of longeron reactions must be zero in the direction perpendicular to M_γ,

$$F_1^y \cos\gamma + \frac{F_3^y}{2}(\cos\gamma - \sqrt{3}\sin\gamma) = 0 \tag{C12}$$

By combining these equations, F_i^y are found to be

$$F_1^y = \frac{M_\gamma}{3R}(\cos\gamma - \sqrt{3}\sin\gamma) \tag{C13}$$

$$F_2^y = \frac{M_\gamma}{3R}(\cos\gamma + \sqrt{3}\sin\gamma) \tag{C14}$$

and

$$F_3^y = -\frac{2M_\gamma}{3R}\cos\gamma \tag{C15}$$

(Note that a positive sign indicates a compressive force, see Figure C2.) Now, by substituting from equation (C9) for M_γ, these equations for F_i^y become

$$F_1^y = \frac{Py_L\ (\cos\gamma - \sqrt{3}\sin\gamma)}{3R\ (1 - p_B^*)} \tag{C16}$$

$$F_2^y = \frac{Py_L\ (\cos\gamma + \sqrt{3}\sin\gamma)}{3R\ (1 - p_B^*)} \tag{C17}$$

and

$$F_3^y = \frac{2Py_L\cos\gamma}{3R\ (1 - p_B^*)} \tag{C18}$$

The lateral inertial load nW has been assumed to act in the direction perpendicular to $\gamma = 0$ (see Figure C2), so as to equally compress longerons (1) and (2) and tension longeron (3). The midspan moment M_O that results from the lateral loading and its deflection is the sum of the moments necessary to equiliberate both nW and the force P. That is,

$$M_O = \frac{nWL}{8} + Py_n \tag{C19}$$

The lateral deflection y_n is caused by nW and P, and this deflection is calculated by approximating the deflection shape due to nW, alone, to be sinusoidal, and then amplifying that deflection by a factor $(1 - p_B^*)^{-1}$, due to the presence of the axial load P. Thus, y_n is approximated as the so-amplified, usual midspan deflection of a laterally loaded beam;

$$y_n = \frac{\frac{5}{384}\frac{nWL^3}{EI_B}}{1 - p_B^*} \tag{C20}$$

The longeron forces F_i^W which provide M_O are derived by setting $\gamma = 0$ in equations (C13), (C14) and (C15);

$$F_1^W = F_2^W = \frac{M_O}{3R} \tag{C21}$$

and

$$F_3^W = -\frac{2M_O}{3R} \tag{C22}$$

By substituting from equation (C19) from M_O and equation (C20) for y_n, F_i^W are determined as

$$F_1^W = F_2^W = \frac{nWL}{24R} + \frac{P\left(\frac{5}{384}\frac{nWL^3}{EI_B}\right)}{3R\ (1 - p_B^*)} \tag{C23}$$

and

$$F_3^W = -\frac{nWL}{24R} - \frac{P\left(\frac{10}{384}\frac{nWL^3}{EI_B}\right)}{3R\ (1 - p_B^*)} \tag{C24}$$

The total load in each longeron, F_i, is found as the sum of the foregoing contributions F_i^P, F_i^Y and F_i^W;

$$F_1 = \frac{P}{3}\left[1 + \frac{\frac{y_L}{R}(\cos\gamma - \sqrt{3}\sin\gamma) + \frac{5\pi^2}{384}\bar{W}\frac{L}{R}p_B^*}{1 - p_B^*} + \frac{\bar{W}}{8}\frac{L}{R}\right] \tag{C25}$$

$$F_2 = \frac{P}{3}\left[1 + \frac{\frac{y_L}{R}(\cos\gamma + \sqrt{3}\sin\gamma) + \frac{5\pi^2}{384}\bar{W}\frac{L}{R}p_B^*}{1 - p_B^*} + \frac{\bar{W}}{8}\frac{L}{R}\right] \tag{C26}$$

and $$F_3 = \frac{P}{3}\left[1 - \frac{\frac{2y_L}{R}\cos\gamma + \frac{\pi^2}{38.4}\bar{W}\frac{L}{R}p_B^*}{1 - p_B^*} - \frac{\bar{W}}{4}\frac{L}{R}\right] \quad \text{(C27)}$$

where $$\bar{W} = \frac{nW}{P} \quad \text{(C28)}$$

The above equations for F_i are used in the following form in the remainder of this analysis:

$$f_i = p_{EU}^* K C_i \quad (i = 1, 2 \text{ and } 3) \quad \text{(C29)}$$

where $$f_i = \frac{F_i}{F_{CR}} \quad \text{(C30)}$$

$$F_{CR} = \frac{\pi^2 EA\rho^2}{\ell^2} \quad \text{(C31)}$$

= longeron buckling strength

ρ = Radius of gyration of longeron cross section

$$p_{EU}^* = \frac{P}{P_{EU}}$$

= ratio of applied load to Euler strength of column

$$P_{EU} = \frac{3\pi^2 EAR^2}{2L^2} \quad \text{(C33)}$$

$$K = \frac{1}{2}\left(\frac{R}{L}\right)^2\left(\frac{\ell}{R}\right)^2\left(\frac{R}{\rho}\right)^2 \quad \text{(C34)}$$

and C_i are the bracketed terms in equations (C25), (C26) and (C27), rewritten in the following form:

$$C_1 = 1 + \frac{\frac{y_L}{R}(\cos\gamma - \sqrt{3}\sin\gamma) + \frac{5\pi^2}{384}\bar{W}\frac{L}{R}\frac{P^*_{EU}}{\bar{P}_B}}{1 - \frac{P^*_{EU}}{\bar{P}_B}} + \frac{\bar{W}}{8}\frac{L}{R} \qquad (C35)$$

$$C_2 = 1 + \frac{\frac{y_L}{R}(\cos\gamma + \sqrt{3}\sin\gamma) + \frac{5\pi^2}{384}\bar{W}\frac{L}{R}\frac{P^*_{EU}}{\bar{P}_B}}{1 - \frac{P^*_{EU}}{\bar{P}_B}} + \frac{\bar{W}}{8}\frac{L}{R} \qquad (C36)$$

and

$$C_3 = 1 - \frac{\frac{2y_L}{R}\cos\gamma + \frac{\pi^2}{38.4}\bar{W}\frac{L}{R}\frac{P^*_{EU}}{\bar{P}_B}}{1 - \frac{P^*_{EU}}{\bar{P}_B}} - \frac{\bar{W}}{4}\frac{L}{R} \qquad (C38)$$

where

$$\bar{P}_B = \frac{P_B}{P_{EU}} = \frac{P}{P_{EU}}\frac{P_B}{P} = P^*_{EU}/P^*_B \qquad (C38)$$

Now consider the axial stiffness of an initially wavy longeron compressed by a force F. From S. Timoshenko, THEORY OF ELASTIC STABILITY, p. 32, the deflection y of an initially wavy longeron when acted upon by axial load F is

$$y = \frac{y_\ell}{1 - f}\sin\frac{\pi x}{\ell} \qquad (C39)$$

where y_ℓ is the amplitude of initial waviness;

$$y_O = y_\ell \sin\frac{\pi x}{\ell} \qquad (C40)$$

and f is defined by equation (C30).

The axial shortening δ_y of the longeron, which results from its deflection, is

$$\delta_y = \frac{1}{2}\int_0^{\ell} (y')^2\, dx - \frac{1}{2}\int_0^{\ell} (y_0')^2\, dx$$

$$= \frac{\pi^2 y_\ell^2}{4\ell}\left[\frac{1}{(1-f)^2} - 1\right] \qquad \text{(C41)}$$

Since the total longeron shortening δ must include that resulting from axial strain,

$$\delta = \frac{\pi^2 y_\ell^2}{4\ell}\left[\frac{1}{(1-f)^2}\right] + \frac{F\ell}{AE} \qquad \text{(C42)}$$

The tangent modulus of total axial shortening of a longeron under load F is

$$E_{TAN} = \frac{\ell}{A}\frac{dF}{d\delta} \qquad \text{(C43)}$$

By taking the indicated derivative of δ in equation (C42),

$$\frac{E}{E_{TAN}} = 1 + \frac{d\delta_y}{df}\frac{df}{dF}$$

$$= 1 + \frac{EA}{\ell}\left[\frac{\pi^2 y_\ell^2}{2\ell}\frac{1}{(1-f)^3}\right]\left(\frac{\ell^2}{\pi^2 EA\rho^2}\right)$$

$$= 1 + \frac{\left(y_{\ell}/\rho\right)^2}{2(1-f)^3} \qquad \text{(C44)}$$

Therefore, this equation for E/E_{TAN} is used for the modulus ratios appearing for the longerons in equation (C4);

$$\frac{E}{E_i} = 1 + \frac{\left(y_{\ell/\rho}\right)^2}{2(1 - f_i)^3} \tag{C45}$$

The previously defined [equation (C38)] buckling strength parameter $\bar{p}_B$ can be expressed in terms of the ratio of the actual bending stiffness [equation (C4)] to the ideal (nonwavy) bending stiffness of the column as follows:

$$\bar{p}_B = \frac{EI_B}{1.5EAR^2}$$

$$= \frac{1}{2}\left[\frac{\frac{E}{E_1}(\sin\gamma + \sqrt{3}\cos\gamma)^2 + \frac{E}{E_2}(\sin\gamma - \sqrt{3}\cos\gamma)^2 + \frac{E}{E_3}4\sin^2\gamma}{\frac{E}{E_1}\frac{E}{E_2} + \frac{E}{E_1}\frac{E}{E_3} + \frac{E}{E_2}\frac{E}{E_3}}\right] \tag{C46}$$

where the ratios E/E_i are determined from equation (C45). Thus, the dependent strength variable $\bar{p}_B$ is expressed, although not explicitly, in terms of the independent loading variable p^*_{EU}, the waviness parameters $\frac{y_L}{R}$ and $y_{\ell/\rho}$, the waviness orientation γ and the geometric parameters (contained in K) [equation (C34)] $\frac{L}{R}$, $\frac{\ell}{R}$ and $\frac{R}{\rho}$. Therefore, nontrivial values of $\bar{p}_B$ can be calculated for assigned values of the independent variables, for $f_i < 1$ [note denominator in equation (C45)].

The buckling strength $\bar{p}_B$ was calculated as it varies with p^*_{EU} for an example case where

$$\gamma = \frac{\pi}{3} \text{ radians}$$

$$\bar{W} = 0$$

$K = 1$ (as for optimum design of a nonwavy column)

In this case, the foregoing equations become

$$\bar{p}_B = \frac{1.5}{\frac{1}{2}\left\{1 + \frac{y_{\ell/\rho}^2}{2\left[1 + p^*_{EU}\left(1 - \frac{y_{L/R}}{1 - \frac{p^*_{EU}}{\bar{p}_B}}\right)\right]^3}\right\} + 1 + \frac{y_{\ell/\rho}^2}{2\left[1 - p^*_{EU}\left(1 + \frac{2y_{L/R}}{1 - \frac{p^*_{EU}}{\bar{p}_B}}\right)\right]^3}} \quad \text{(C47)}$$

The solutions to this equation are shown in Figure C3 as a graph of $\bar{p}_B$ versus p^*_{EU} for $y_\ell/\rho = 0.10$ and various values of $y_{L/R}$. These solutions show the following:

1. When $y_L/R = 0$, $p^*_{EU} = \bar{p}_B$. That is, the maximum load that the column can withstand is equal to its conventional buckling strength, as reduced from its ideal Euler strength to account for effects of longeron initial waviness.

2. When $y_L/R \neq 0$, the maximum loading p^*_{EU} that the column can withstand, p^*_{MAX}, is less than the classical buckling strength $\bar{p}_B$. In this instance, the maximum strength p^*_{MAX} is <u>not</u> caused by buckling, a bifurcation of stable and unstable equilibria. Instead, it is a structure for which any attempt to increase its loading from

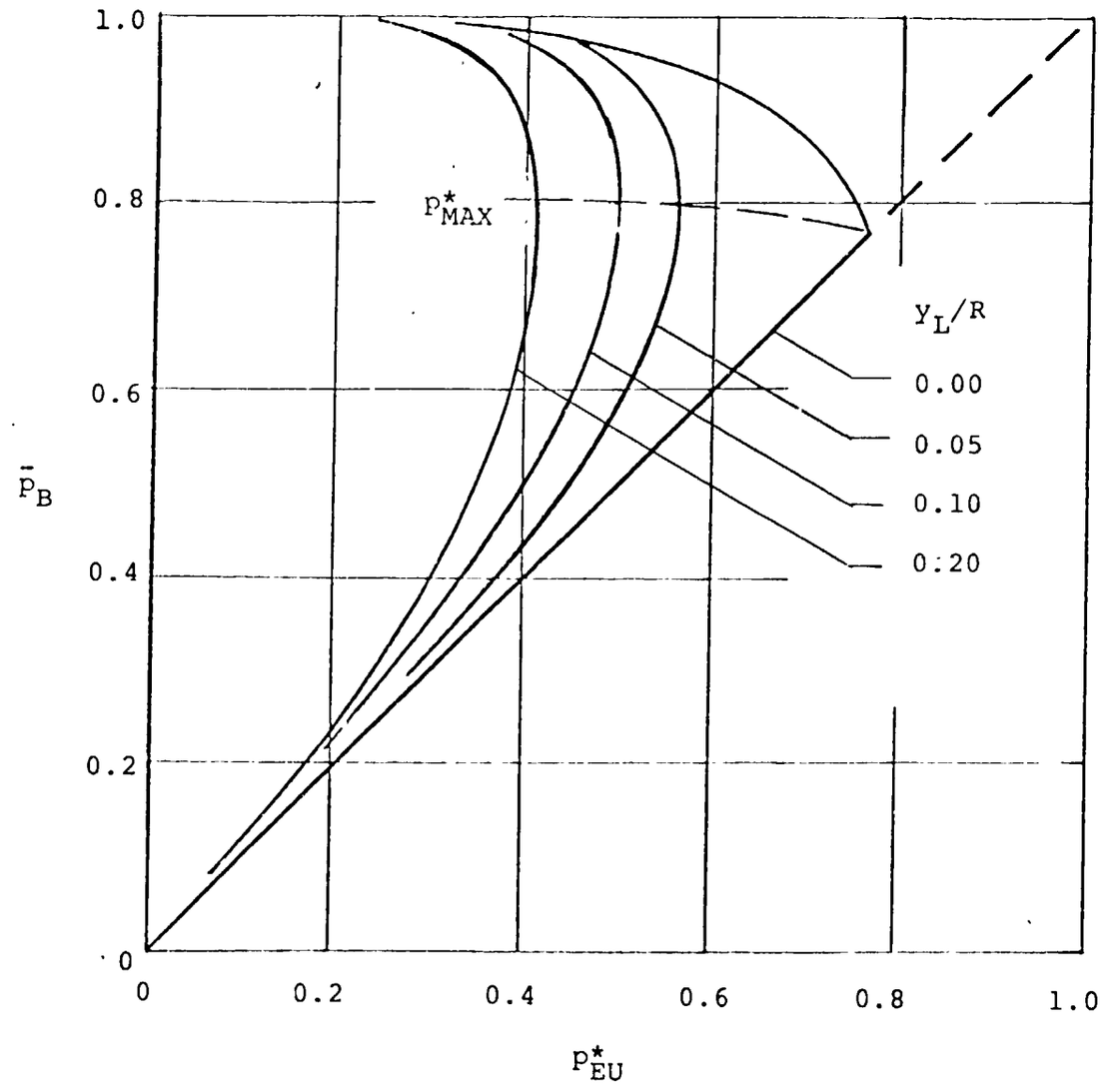

FIGURE C3 -- Buckling Strength $\bar{p}_B$ as It Varies with Applied Load p^*_{EU} for Various Overall Waviness y_L/R ; $y_\ell/\rho = 0.10$

p^*_{MAX} only results in unstably decreasing its bending stiffness and increasing its deflection. That is, only one state of equilibrium exists, and it is unstable when $p^*_{EU} < p^*_{MAX}$ and $\bar{p}_B <$ its value at p^*_{MAX} .

Figure C4 shows the dependence of p^*_{MAX} on waviness parameters y_L/R and y_ℓ/ρ for this example case. It is evident that the presence of only small amounts of either type of waviness significantly reduce p^*_{MAX} from unity. However, when these wavinesses are large, p^*_{MAX} is less sensitive to small changes in those wavinesses.

Regarding the effects of the direction in which the column is wavy, it was determined for an example case where $\bar{W} = 0$, $K = 1$ and y_L/R and y_ℓ/ρ were constant, that p^*_{MAX} is minimized when the column waviness is in a direction perpendicular to $\gamma = 60° (1 - 2n)$, $n = 0$, 1 , $2 \ldots i$. And p^*_{MAX} is maximized when the waviness is perpendicular to $\gamma = 60° (2n)$. The difference between these extrema of p^*_{MAX} can be large for large values of y_L/R and y_ℓ/ρ , but there is no difference when $y_L/R = 0$. Further, the angles γ at which these extrema occur will change from those noted when $\bar{W} \neq 0$, and the differences in extrema also vary with K .

No further investigation of γ-effects are investigated here, since this appendix is intended only to present the strength analysis and pertinent parameters for wavy columns. However, γ-effects for the Solar Sailer application are discussed in the body of this report.

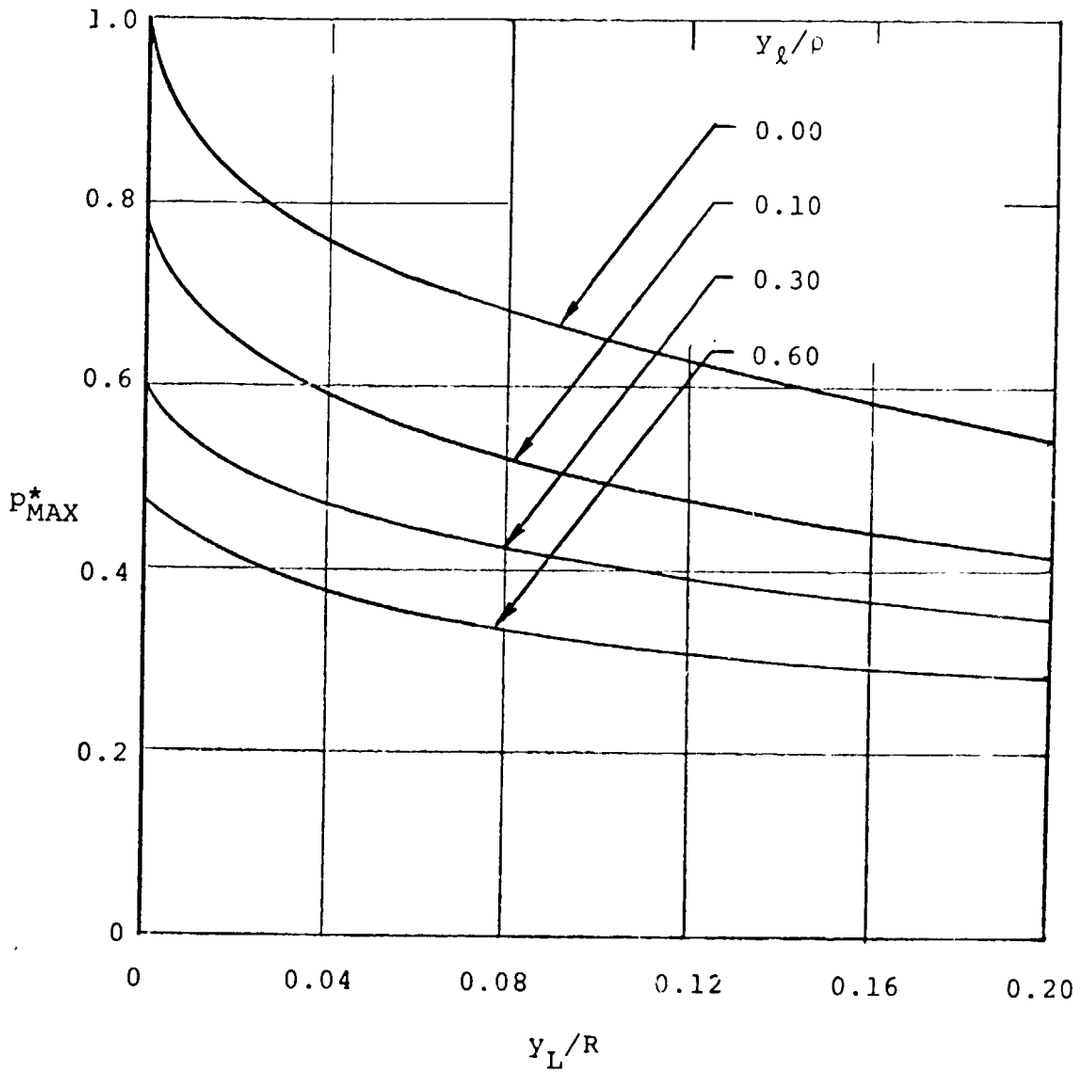

FIGURE C4 -- Maximum Compressive Strength of Column Versus Waviness Parameters y_ℓ/o and y_L/R ; K = 1 and $\bar{w} = 0$.